CERTIFICATION OF APPROVAL

Removal of Carbon Dioxide from Natural Gas by Using Gas Hydration

by

Vu Thi Huong

A project dissertation submitted to the

Chemical Engineering Programme

Universiti Teknologi PETRONAS

in partial fulfillment of the required for the

BACHELOR OF ENGINEERING (Hons)

(CHEMICAL ENGINEERING)

Approved by.

_____
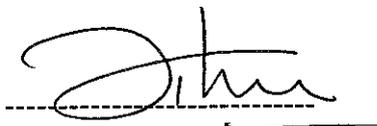
(Dr. Hilmi Bin Mukhtar)

Project Supervisor

Universiti Teknologi PETRONAS

Tronoh, Perak

November 2004

i

CERTIFICATION OF ORIGINALITY

This is to certify that I am responsible for the work submitted in this project, that the original work is my own except as specified in the references and acknowledgments, and that the original work contained herein have not been undertaken or done by unspecified source or persons.
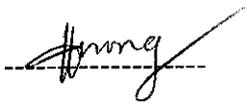
Vu Thi Huong

ABSTRACT

Natural Gas is a vital component of the world's supply of energy. It is one of the cleanest, safest, and most useful of all energy sources. Natural gas has many uses, residentially, commercially and industrially.

Carbon dioxide is a corrosive and non-combustible gas present in natural gas. This undesired gas must be removed from natural gas to a permissible level. Typical pipeline quality states that the composition of carbon dioxide in the treated gas stream must not be more than 2%. In Malaysia, Gas Malaysia set an even more stringent limit where the level of carbon dioxide is further reduced to 1.83% maximum.

A typical content of 0-8% carbon dioxide can be removed by using commercially available absorption or membrane method. However, with carbon dioxide content increased to 50-80% in natural gas produced, the current equipments can not purify this much of carbon dioxide effectively. Therefore gas hydration is being studied by mathematical method and simulation to see the possibility of applying this property of gases to purify natural gas.

Hydrates are ice-like solids that form when a sufficient amount of water and a hydrate former is present, and there is a right combination of temperature and pressure (hydrate formation is favored by low temperature and high pressure). Hydrates are notorious for forming at conditions where a solid would no otherwise be expected.

Methane and carbon dioxide clathrates occur naturally at temperature above freezing point of water (up to 30°C) under pressure of 0.1 MPa (~1atm) to 100 MPa (~1000atm). Different types of gases form hydrate at different ranges of temperature and pressure. Gas hydrate can be converted back to gas and water easily by applying heat to the hydrate solid. This property can be employed to the separation of carbon dioxide from natural gas by either capturing carbon dioxide or methane in hydrate form if applicable.

The main objective of this study is to predict the separation of carbon dioxide from methane using hydration method. The effect of associated parameters such as temperature and pressure are also included.

PetronasSim 2.55.2, Excel and K-factor methods were used in this work to obtain hydrate formation temperature and pressure, and phase equilibrium composition. The results show that: As temperature increases, formation pressure increases; as carbon content of gas mixture increase, formation pressure decreases; as water/gas ratio increases, formation pressure increases; At low temperature more carbon dioxide form hydrate as compared to methane; At low pressure region (associated with low temperature) the higher the pressure the lower the concentration of carbon dioxide in vapor phase or the more carbon dioxide form hydrate Temperature, pressure and gas composition are main parameters governing the formation of gas hydrate; The lower is the temperature the larger is the difference of concentration of carbon dioxide in hydrate phase and in vapor phase which indicates a better separation;

The study shows that gas hydration has a bright future to be explored further to transform the theory into designing equipments to separate carbon dioxide from natural gas.

ACKNOWLEDMENTS

TABLE OF CONTENTS

LIST OF ILLUSTRATION

ABBRIVIATIONS AND NOMENCLATURES

P = pressure. [bar]

T = temperature. [K, ^{o}F]

V_m = specific volume [m^3/kmol]

R = gas constant = 0.08314 [m^3.bar/kmol.K]

a = van der Waals constant. $\left[\left(\dfrac{m^3}{kmol}\right)^2\right]$

b = van der Waals constant. $\left[\dfrac{m^3}{kmol}\right]$

K_i, = distribution ratio of the component between the gas and the hydrate [-]

y_i = mole fraction of component i in vapor phase [-]

s_i = mole fraction of component i in hydrate phase. [-]

Π = pressure [psia]

A, B…R are constants given in table 2.2

z_i = composition of the feed [-]

V = vapor phase fraction [-]

w/g = water/gas ratio [-]

CHAPTER 1

INTRODUCTION

1.1 Background of Study

Natural Gas is a vital component of the world's supply of energy. It is one of the cleanest, safest, and most useful of all energy sources. Natural gas has many uses, residentially, commercially, and industrially.

Natural gas is colorless, shapeless, and odorless in its pure form. Quite uninteresting - except that natural gas is combustible, and when burned it gives off a great deal of energy. Unlike other fossil fuels, however, natural gas is clean burning and emits lower levels of potentially harmful byproducts into the air.

Natural gas is a combustible mixture of hydrocarbon gases. While natural gas is formed primarily of methane, it can also include ethane, propane, butane and pentane. The composition of natural gas can vary widely, but below is a chart outlining the typical makeup of natural gas before it is refined.

Table 1.1: Typical composition of natural gas.

Methane	CH_4	70-90%
Ethane	C_2H_6	0-20%
Propane	C_3H_8	
Butane	C_4H_{10}	
Carbon Dioxide	CO_2	0-8%
Oxygen	O_2	0-0.2%
Nitrogen	N_2	0-5%
Hydrogen sulfide	H_2S	0-5%
Rare gases	A, He, Ne, Xe	trace
Metals	Hg, Radioactive substances	trace

Natural gas, as it exists underground, is not exactly the same as the natural gas that comes through the pipelines to our homes and businesses. Natural gas, as we use it, is almost entirely methane. Natural gas found underground, however, can come associated with a variety of other compounds and gases, as well as oil and water, which must be removed.

Carbon Dioxide (CO_2) is a well known acid gas that is present in the natural gas. In enhanced oil well recovery (EOR) application, the gas is pumped into depleting oil reserves at high pressures to drive residual oils to existing oil wells. Over an extended period of time, the CO_2 gas mixed with the natural gas associated with the wells and can reach as high as 95% (Spillman, 1989). The composition of CO_2 in the existing natural gas wells varies for different geographical locations. Its composition can reach as high as 80% in certain natural gas wells (Rojey et al., 1997). Table 1.2 shows the composition of CO_2 in some natural gas wells in the world.

Table 1.2: Composition of CO_2 in some natural gas wells (Rojey et al., 1997).

No.	Location	Composition (%)
1	Lacq, France	9.3
2	Frigg, Norway	0.3
3	Uch, Pakistan	46.2
4	Kapuni, New Zealand	43.8
5	Uthmaniyah, Saudi Arabia	8.9
6	Terengganu, Malaysia	7.0
7	Krecsegopan, Poland	83.0
8	North German Plain, Germany	60.0
9	Kirkuk, Iraq	7.1
10	Duri, Indonesia	23.0

Due to its acidic nature and being non-combustible, CO_2 in the natural gas must be removed to a permissible level. Typical pipeline quality states that the composition of CO_2 in the treated gas stream must not be more than 2% (Spillman, 1989). In Malaysia,

Gas Malaysia set an even more stringent limit where the level of CO_2 is further reduced to 1.83% maximum.

A typical content of 0-8% carbon dioxide can be removed by using commercially available absorption or membrane method. However, with carbon dioxide content increased to 50-80% in natural gas produced, the current equipments can not purify this much of carbon dioxide effectively therefore gas hydration method is studied to see possible solution.

The tendency of certain gases to form solid compounds with water at low temperatures and moderate pressures has been known for nearly 200 years (Sloan,1998), but these compounds were largely of academic interest until the oil and gas industry recognized that gas hydrate formation under certain conditions can block pipelines. This discovery motivated structural studies of methane and other gases (Hollander et al., 1997 and Von Stackelberg, 1949), which revealed to them as gas clathrates, or 'guest-host' inclusion compounds. The 'host' lattice consists of an ice-like hydrogen-bonded network of water molecules with polyhedral cavities large enough to accommodate a variety of 'guest' molecules.

Different types of gases form hydrate at different ranges of temperature and pressure. Gas hydrate can be converted back to gas and water easily by applying heat to the hydrate solid. This property can be employed to the separation of carbon dioxide from natural gas by either capturing carbon dioxide or methane in hydrate form if applicable.

1.2 Problem Statement
1.2.1 Problem Identification

Carbon dioxide is a corrosive and non-combustible gas present in natural gas. This undesired gas must be removed from natural gas to a permissible level. Typical pipeline quality states that the composition of carbon dioxide in the treated gas stream must not

be more than 2% (Spillman, 1989). In Malaysia, Gas Malaysia set an even more stringent limit where the level of carbon dioxide is further reduced to 1.83% maximum.

A typical content of 0-8% carbon dioxide can be removed by using commercially available absorption or membrane method. However, with carbon dioxide content increased to 50-80% in natural gas produced, the current equipments can not purify this much of carbon dioxide effectively. Therefore gas hydration is being studied by simulation to see the possibility of applying this property of gases to design a hydrator which can purify natural gas.

1.2.2   Significant of the Project

This is a preliminary research on the feasibility of applying gas hydration knowledge in separation of carbon dioxide and methane mixture.

1.3 Objective and Scope of Study
1.3.1   Scope of Study

In this study, hydrate technology will be explored to find an efficient separation method for purifying natural gas. The study focuses on gathering thermodynamic data of carbon dioxide hydrate and methane hydrate, and manipulation operation parameters such as temperature, pressure, carbon dioxide composition in feed gas stream, water-gas ratio, and hydrate formation ratio.

1.3.2 Objectives

The objectives of this study can be summarized as follows:

a. To explore the possibility of forming gas hydrate to remove carbon dioxide from carbon dioxide-methane mixture.

b. To study parameters governing the formation of gas hydrate.

c. To select the best operating condition for methane-carbon dioxide separation

1.3.3 The Relevancy of the Project

The project provides a summary of understanding about gas hydrates (mainly carbon dioxide and methane hydrates). It also gives the simulation steps to obtain hydrate temperature and pressure formation in PetronasSim and calculation steps to obtain phase equilibrium composition of hydrate formation. A set of data for hydrate temperature and pressure formation, and phase equilibrium composition was generated at temperature from -10 to $10^{\circ}C$; pressure from 293.7 to 7322.66 kPa; water/gas ratio of 1, 3, 5.75, 7; carbon dioxide content of 0, 10, 20, 30, 40, 50, 60, 70, 80, 100%.

1.3.4 Feasibility of the Project within the Scope and Time frame

Due to time constraint of one semester individual project, the study focuses only on the mixture of carbon dioxide and methane. The project was completed successfully within the time frame.

In chapter 2, detail information about gas hydrates (theirs structure composition, formation condition, global reserve estimation, history, and occurrence), equations of state and K-Factor method will be presented.

5

CHAPTER 2
LITERATURE REVIEW

2.1 What are Gas Hydrates (Clathrates)?

Hydrates are ice-like solids that form when a sufficient amount of water and a hydrate former is present, and there is a right combination of temperature and pressure (hydrate formation is favored by low temperature and high pressure). Hydrates are notorious for forming at conditions where a solid would no otherwise be expected. Water is called the "host" and it forms a hydrogen-bonded lattice; a three-dimensional cage-like structure. The hydrate former, called the "guest", enters the lattice and stabilizes it. The stabilized lattice precipitates as a solid.

The nature of the equilibrium in the hydrate region depends upon the amount of water present. A large amount of water means the equilibrium is between water and the hydrate. A small amount of water means the equilibrium is between a gas and the hydrate. If there is an extreme amount of water, then the hydrate does not form at all, even though the conditions are in the "hydrate" region. If the mixture is very lean in water, no hydrate forms even though the conditions are in the "hydrate" region. Free water needs not be present for a hydrate to form. Figure 2.1 and 2.2 shows the picture of methane hydrate grows in volume of water and gas.

Figure 2.1: Whiskery methane hydrate growing in volume of gas and water and soft-gel crystals (marked by an arrow) growing in volume of water. (P = 83 atm (8.41 MPa); T = 275.9 K (2.75 °C)) (Makogon, 1997)
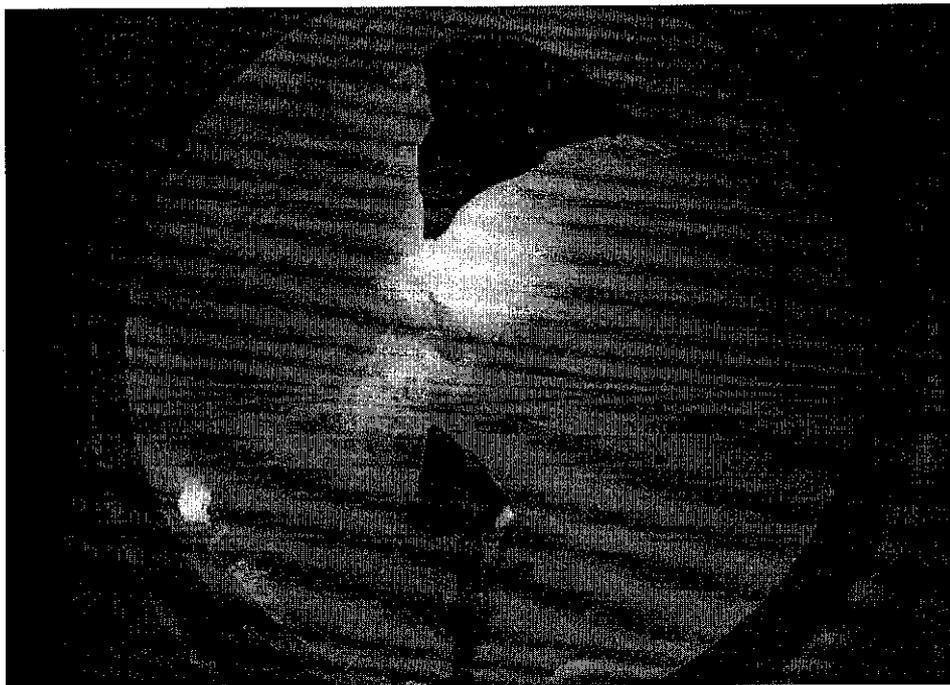
Figure 2.2: Whiskery crystals of methane hydrate, growing in a gas volume (P = 87 bar (8.7 MPa); T = 275.1 K (1.95 °C)) (Makogon, 1997)

Hydrates are basically of three types called Type I, Type II, and Type H. Other types of hydrates are known and proposed, but they are uncommon. The crystal structures of hydrates are three-dimensional and are quite complicated. This project only concerns with Type I. It is usually smaller molecules form Type I hydrates. Type I hydrate formers include: (1) methane, (2) ethane, (3) carbon dioxide, and (4) hydrogen sulfide. Type I hydrates are made up of 8 polyhedral cages -- 6 large ones and 2 small (Figure 2.3). They are made up of 46 water molecules and thus have a theoretical composition of $8X \cdot 46\ H_2O$ or $X \cdot 5\ 3/4\ H_2O$, where X is the guest molecule.
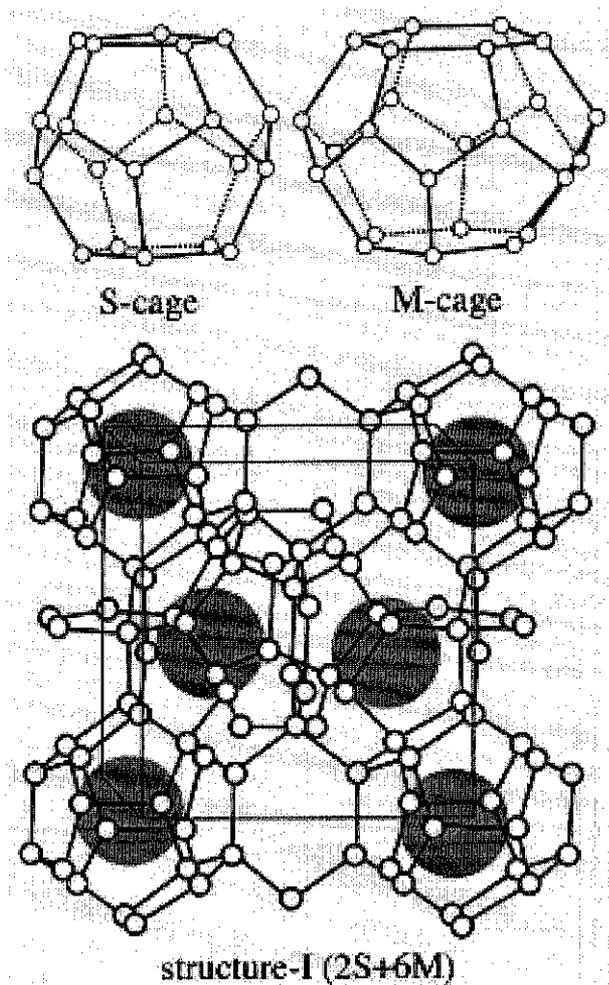
Figure 2.3: Structure I of Clathrates

Figure 2.4 shows the hydrate loci for several components in natural gas. At temperatures less than the loci and at pressure greater than the loci (i.e., to the left and above) are where hydrates will form. For example, at 5°C and 1 MPa, hydrogen sulfide, ethane and propane form hydrates, whereas carbon dioxide, methane, and isobutane do not.
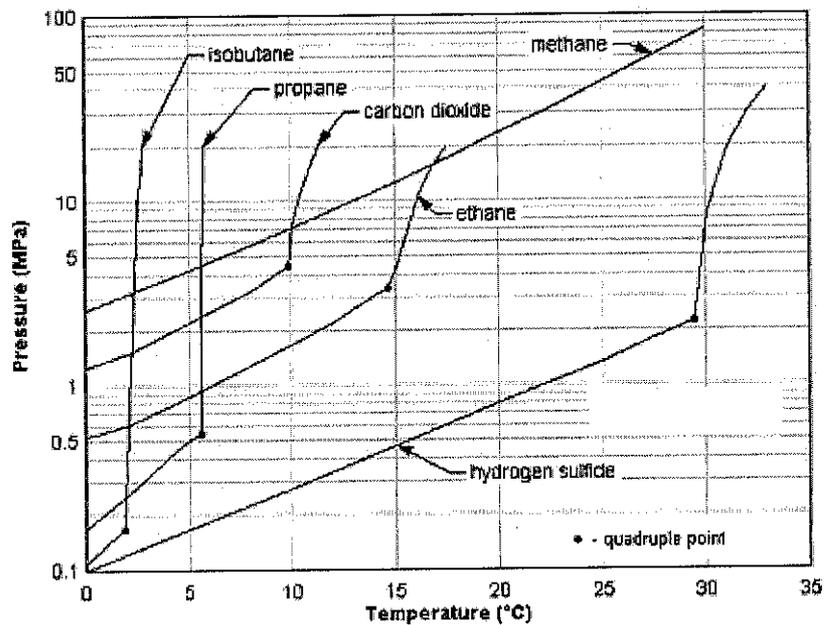
Figure 2.4: Hydrate loci for several components found in natural gas (Carroll, 1999)

Both technogenic and natural gas hydrates form, stably exist, and decomposed in a very broad range of temperatures. A temperature range below 0°C is very important during development if hydrocarbon deposits in the Artic regions, in several gas processing technologies, and in the solution of outer space. Figure 2.5 presents the equilibrium curves for hydrates of several gases at temperatures below 0°C.

9
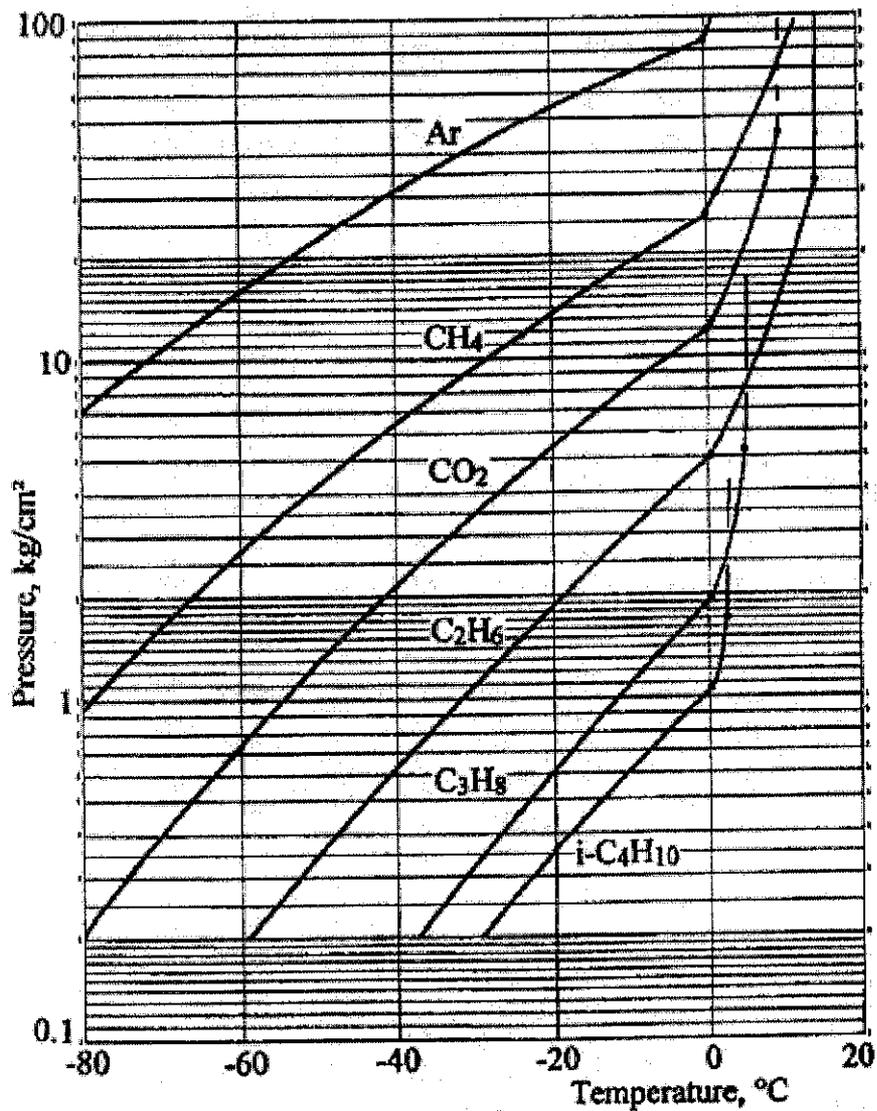
Figure 2.5: Hydrate formation with different gases at T <0 °C. (Makogon, 1997)

The phase behavior of hydrocarbon + water mixture differs significantly from that of normal hydrocarbon mixtures. Differences arise from two effects, both of which have their basis in hydrogen bonding. First, the hydrate phase is a significant part of all hydrocarbon + water phase diagrams for hydrocarbons with a molecular size lower than 9 Angstroms. Secondly, water and hydrocarbon molecules are so different that, in the condensed state, two distinct liquid phases form, each with a very low solubility in the other. Figure 2.6 represents the phase diagram for some simple gases found in natural gas.

10
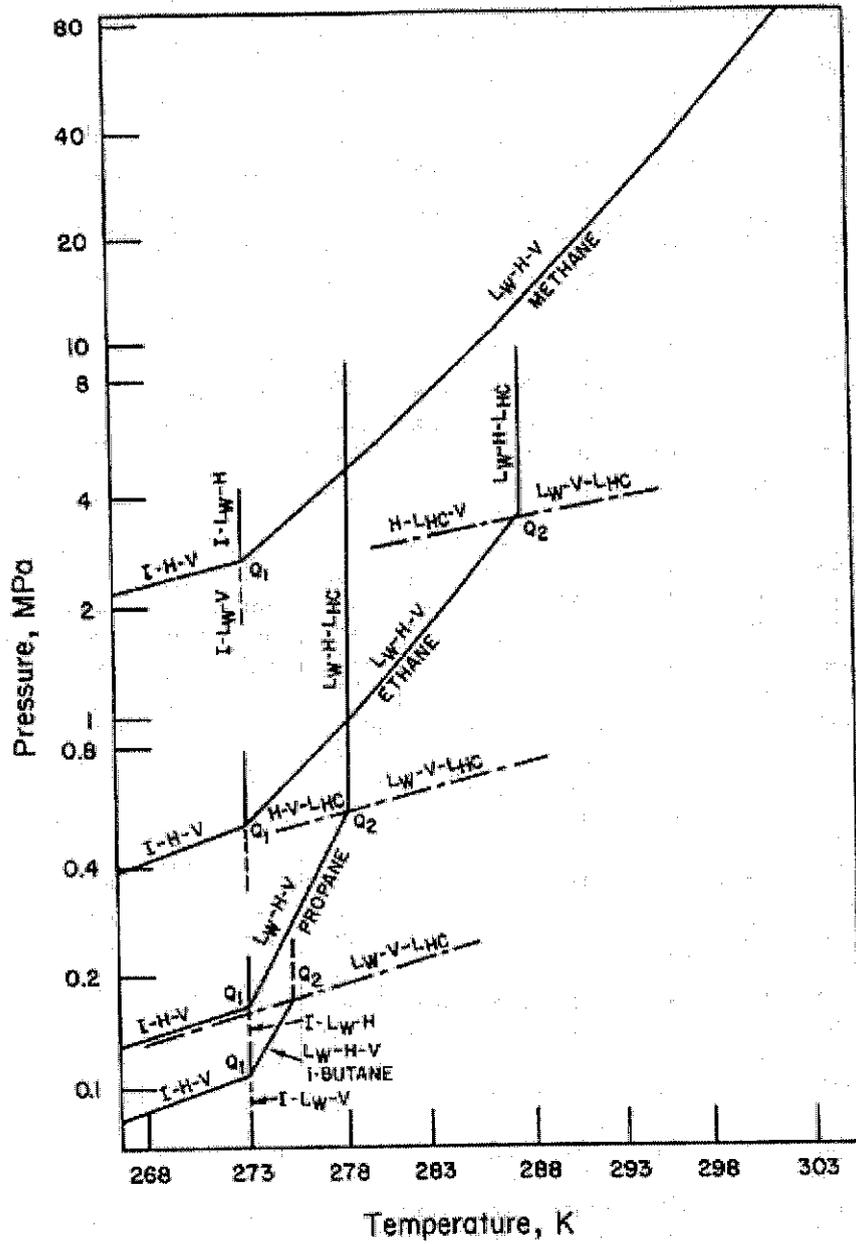
Figure 2.6: Phase diagrams for some simple natural gas hydrocarbons which form hydrates. (Sloan, 1997)

Table 2.1 shows the critical temperature and pressure as well as hydrate formation quadruple points for methane and carbon dioxide.

Table 2.1: Parameters of quadruple points of methane and carbon dioxide. (Makogon, 1997)

Gas	Molecular diameter, nm	Critical		Quadruple Points							
		P, MPa	T, K	I		II		III		IV	
				P, MPa	T, K	P, MPa	T, K	P, MPa	T, K	P, MPa	T, K
CH_4	0.436	4.6	190.75	2×10^{-9}	36	2.563	272.9	-	-	1650	331
CO_2	0.512	7.382	304.19	5×10^{-6}	121	1.256	273.1	4.499	283.1	900	287

2.2 Global estimation of natural gas hydrate

It is generally assumed that oceanic gas hydrates contain a huge volume of natural gases, mainly methane. The most widely cited estimate of global hydrate-bound gas is 21×10^{15} m^3 of methane at STP (or ~10,000 Gt of methane carbon), which is proposed as a "consensus value" from several independent estimations. This large gas hydrate reservoir is further suggested as an important component of the global carbon cycle and as a future energy source. It appears that the global estimates of hydrate-bound gas decreased by at least one order of magnitude from 1970s–early 1980s (estimates on the order of 10^{17}–10^{18} m^3) to late 1980s–early 1990s (10^{16} m^3) to late 1990s–present (10^{14}–10^{15} m^3). The decrease of estimates is a result of growing knowledge of the distribution and concentration of gas hydrates in marine sediments and ongoing efforts to better constrain the volume of hydrate-bearing sediments and their gas yield. These parameters appear to be relatively well constrained at present through DSDP/ODP drilling and direct measurements of gas concentrations in sediments. The global estimate of hydrate-bound gas that best reflects the current knowledge of submarine gas hydrate is in the range $(1–5) \times 10^{15}$ m^3 (~500–2500 Gt of methane carbon) (Milkov, 2003). A significantly smaller global gas hydrate inventory implies that the role of gas hydrates in the global carbon cycle may not be as significant as speculated previously. Gas hydrate may be considered a future energy source not because the global volume of

that it could exist in sizeable quantities in nature. However, a string of discoveries, first in Polar Regions and then spreading throughout the deep-water shelves of every continent, has revealed that natural methane hydrate occurs on a truly staggering scale.

In many areas, the existence of natural methane hydrate is inferred only from indirect evidence obtained through geophysical surveys or geochemical analyses of sediment samples. However, there are a growing number of localities where detailed information is being collected. Each of these localities, with their own unique geologic settings, is unveiling surprising information that questions the initial theories of hydrate formation and ultimately advances the general state of knowledge of natural gas hydrate. Figure 2.7 shows the distribution of natural gas hydrate world wide.
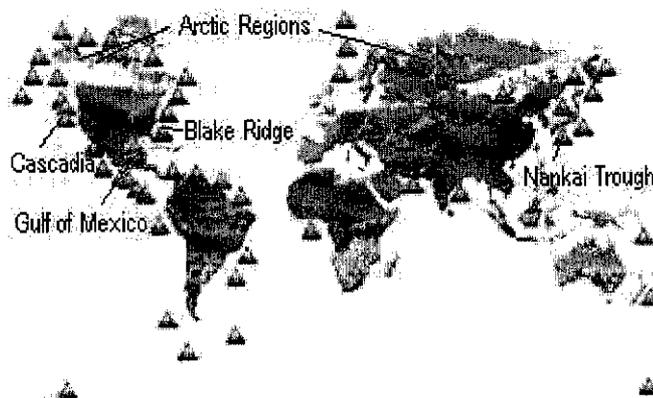
Figure 2.7: Methane Hydrate world wide.

A prime locality for the study of natural methane hydrate is within the Arctic Regions of North America. Although hydrates associated with permafrost contain only a small fraction of the global methane hydrate resource, areas like the North Slope of Alaska provide excellent opportunities to study natural hydrates by combining the data gained from more than two decades of well drilling with relative ease of access. In 1998, the Mackenzie River Delta of Canada's Northwest Territories was the site of the world's first research well drilled specifically to study natural methane hydrate. The Messoyahka gas field of the West Siberia basin is another well-known example of an

arctic hydrate accumulation. Hydrate was inferred from well logging and other data during initial drilling of the field in 1964 and debate continues as to whether dissociation of the hydrate in response to production of deeper free gas zones has resulted in actual production of methane from hydrate.

Perhaps the best-known and most closely studied oceanic hydrate locality is the Blake Ridge, a large pile of deep-water sediment located off the eastern coast of North America. The Blake Ridge has been scanned and probed regularly since the first evidence of hydrate was collected there in the early 1970s. The Blake Ridge's uniform sediment makes it an ideal laboratory for fine tuning the tools and techniques that will be used to study hydrate accumulations around the globe.

A third prominent locality for hydrate occurrence is the deep-water Gulf of Mexico. Unlike the Atlantic shore, the Gulf is an area of significant production of conventional oil and gas. The hazards that unintentional hydrate dissociation pose for drill rigs, pipelines, and other equipment is a prime driver for focused study of hydrates in the Gulf. The significant geologic differences that exist between the Blake Ridge and the Gulf result in the presence of unique features, including visible mounds of hydrate directly on the sea floor. In recent years, scientists have visited the deep gulf in submersible vehicles to observe and sample the mounds. Among the many discoveries are unique chemosynthetic communities, including previously unknown species called ice worms that derive sustenance not from the sun, but directly from the methane slowly dissociating from the hydrate.

In 1999, Japan's Nankai trough region was the target of the first well drilled specifically to test the resource potential of oceanic hydrate. The geologic setting (a subduction zone), characterized by the close proximity of deep water to the land and the resultant improved reservoir character of the sediment, may eventually result in the Nankai region being the host to the first attempts at commercial methane production from hydrate. Examination of a similar tectonic setting on the Pacific coast of North America has resulted in identification of a promising hydrate locality named "Hydrate Ridge", located offshore Oregon. Hydrate Ridge was recently ranked the most important marine

hydrate site for scientific study, and therefore will be a prime focus of an upcoming leg of the Ocean Drilling Project.

Many other regions have also been appraised to various extents, including offshore Alaska, Antarctica, Nigeria, the South China Sea, Norway, Peru, and Australia. As information becomes available on these areas, we will post specific pages for each new site.

2.5 Equations of state

There are a number of equations of state relating pressure, molar or specific volume, and temperature for equilibrium states of substances. Each equation of state valid at different range of temperature and pressure and phases exist at equilibrium as well as the required accuracy. The more accurate prediction needs more complicated equation of state. The equations of state that were studied include: Van de Waals, Redlich-Kwong, Soave-Redlich-Kwong, Peng-Robinson equation.

Van der Waals equation (2-1) is the simplest form of real gas equation of state which works well at temperature above critical temperature, T_c of a substance (Michael et al., 1999). It is inaccurate at vicinity of the critical point as well as other regions. There fore it is definitely not applicable at hydrate forming condition.

$$\left(P + \frac{a}{V_m^2}\right)(V_m - b)) = RT \qquad (2\text{-}1)$$

where P = pressure, bar; T = temperature, K; V_m = specific volume, m^3/kmol ; R = gas constant = 0.08314 m^3.bar/kmol.K; a and b are constants, $\left(\dfrac{m^3}{kmol}\right)^2$ and $\dfrac{m^3}{kmol}$, .

16

Redlich-Kwong equation (2-2) is more accurate than Van der Waal equation at higher temperature. However it is still simple and performs poorly with respect to liquid phase, therefore it is not accurate for calculating vapor-liquid equilibrium. It is only adequate when P/P_c less than one half of T/T_c.

$$P = \frac{RT}{V_m - b} - \frac{a}{V_m(V_m + b)T^{1/2}}$$

(2-2)

Soave-Redlich-Kwong equation (2-3) is a modified form of Redlich-Kwong equation which replaces $a/T^{1/2}$ by $a(T)$ to fit vapor pressure data of hydrocarbons and perform fairly well for these materials.

$$P = \frac{RT}{V_m - b} - \frac{a(T)}{V_m(V_m + b)}$$

(2-3)

The Peng-Robinson Equation (2-4) was developed in 1976 in order to satisfy the following goals:

1. The parameters should be expressible in terms of the critical properties and the acentric factor.

2. The model should provide reasonable accuracy near the critical point, particularly for calculations of the Compressibility factor and liquid density.

3. The mixing rules should not employ more than a single binary interaction parameter, which should be independent of temperature pressure and composition.

4. The equation should be applicable to all calculations of all fluid properties in natural gas processes.

$$P = \frac{RT}{V_m - b} - \frac{a(T)}{V_m(V_m + b) + b(V_m - b)}$$

(2-4)

17

For the most part the Peng-Robinson equation exhibits performance similar to the Soave-Redlich-Kwong equation, although it is generally superior in predicting the liquid densities of many materials, especially nonpolar ones.

Both Soave-Redlich-Kwong and Peng-Robinson equation are possible candidate for the calculation of hydrate phase equilibrium as long as solid phase does not play significant role.

2.6 K-Factor Method

K-Factor method originated with Carson and Katz (1942), although additional data and charts have been reported since then (John Carroll, 2003). On of the ironies of this method is that the original charts of Carson and Katz (1942) have been reproduced over the years even though they were originally marked as "tentative" by the authors. K-factor is defined as the distribution of the component between the hydrate and the gas:

$$K_i = \frac{y_i}{s_i} \tag{2-5}$$

where y_i and s_i are the mole fractions of component i in the vapor and hydrate, respectively. These mole fractions are on a water-free basis, and water is not included in the calculations. It is assumed that sufficient water is present to form hydrate. A chart is available for each of the components commonly encountered in natural gas that is a hydrate former: methane, ethane, propane, isobutane, n-butane, hydrogen sulfide, and carbon dioxide. All nonformers are simply assigned a value of infinity. This is true by definition because $s_i=0$ for nonformer, so there is no nonformer in the hydrate.

2.6.1 K-value

The evaluation of K value for CH_4 and CO_2 can be done using the proposed formula given by Sloan, 1997 as:

$$\ln(K_{vsi}) = A + B*T + C*\Pi + D*T^{-1} + E*\Pi^{-1} + F*\Pi*T + G*T^2 + H*\Pi^2 + I*\Pi*T^{-1} +$$
$$J*\ln(\Pi*T^{-1}) + K*(\Pi^{-2}) + L*T*\Pi^{-1} + M*T^2*\Pi^{-1} + N*\Pi*T^{-2} + O*T*\Pi^{-3} + P*T^3 \qquad (2\text{-}6)$$
$$+ Q*\Pi^3*T^{-2} + R*T^4$$

where Π = pressure, psia; T = temperature, °F; A, B...R are constants given in table 2.2

The above equation was used to fit all of the K value for ,methane K chart and carbon dioxide K chart as shown in figures 2.8 and 2.9 below.
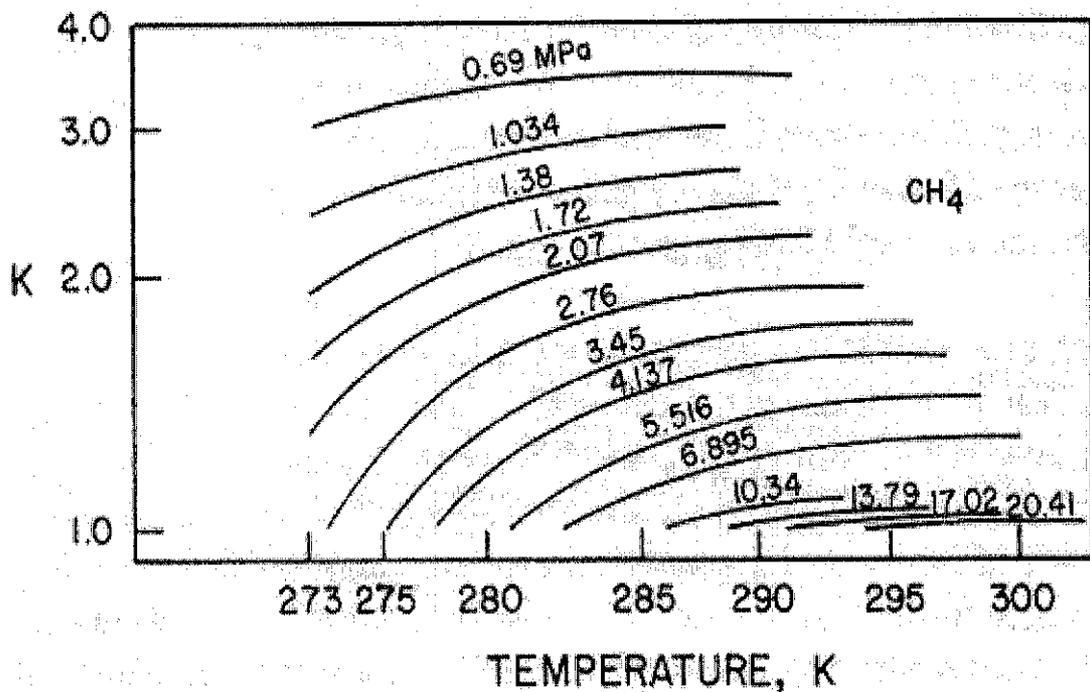
Figure 2.8: Methane K_{vs} Chart. (Sloan, 1997)

19
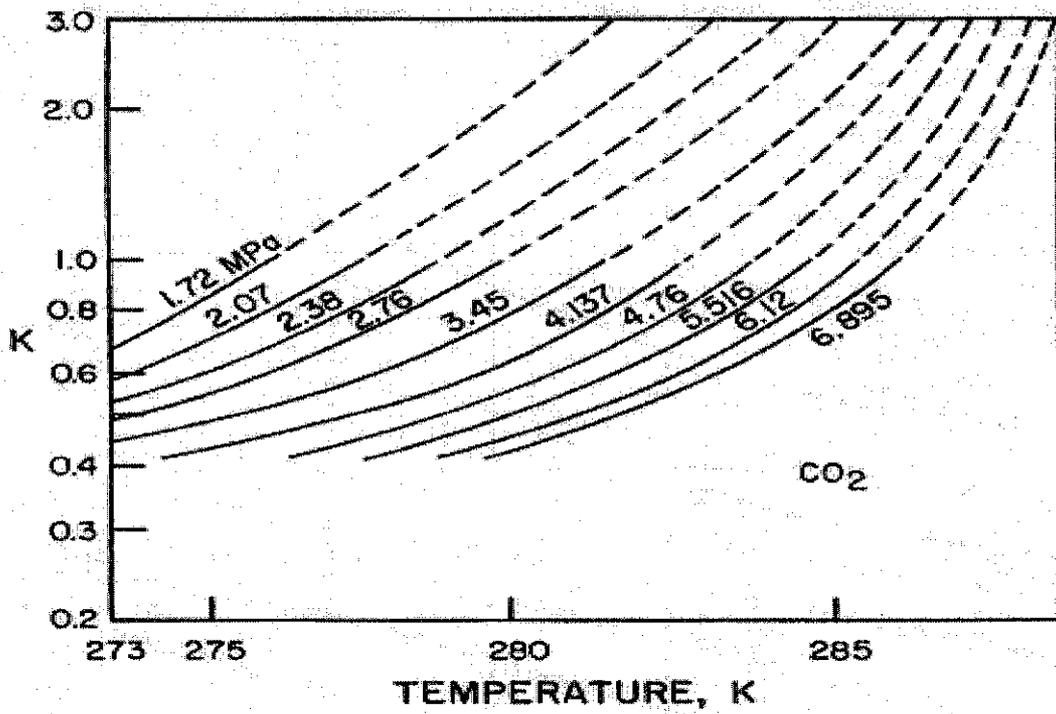
Figure 2.9: Carbon dioxide K_{vs} Chart. (Sloan, 1997)

Table 2.2: Parameters and Accuracy of Prediction of Equation (2-2).

	CO_2	CH_4
A	9.0242	1.63636
B	0	0
C	0	0
D	-207.033	31.6621
E	0	-49.3534
F	4.66E-5	-5.31E-6
G	-6.992E-3	0
H	-2.89E-6	0
I	-6.223E-3	0.128525
J	0	-0.78338
K	0	0
L	0	0
M	0.27089	0
N	0	-5.3569
O	0	0
P	8.82E-5	-2.3E-7
Q	2.55E-6	-2.0E-8
R	0	0
Correl. Coeff	0.996	0.999

2.6.2 Calculation Algorithms

The K-charts are usually used in three methods: (1) given the temperature and pressure, calculate the composition of the coexisting phases; (2) given the temperature, calculate the pressure at which the hydrate forms and the composition of the hydrate; and (3) given the pressure, calculate the temperature at which the hydrate forms and the composition of the hydrate.

a) Flash

The first type of calculation is basically a flash. In this type of calculation, the objective is to calculate the amount of the phases present an equilibrium mixture and to determine the composition if the coexisting phases. The temperature, pressure, and compositions are the input parameters.

The objective function to be solved, in the Rachford-Rice-form, is:

$$f(V) = \sum \frac{z_i(1-K_i)}{1+V(K_i-1)} = 0 \tag{2-7}$$

where z_i is the composition of the feed on a water-free basis. An iterative procedure is used to solve for the vapor phase fraction, V, such that the function equals to zero.

Once the phase fraction has been calculated, the vapor phase can be calculated as follows:

$$y_i = \frac{z_i K_i}{1+V(K_i-1)} \tag{2-8}$$

and from the vapor phase, the composition of the solid phase is calculated from:

$$s_i = \frac{y_i}{K_i} \tag{2-9}$$

b) Incipient Solid Formation

The other two methods are incipient solid formation points and are basically equivalent to a dew point. This is the standard hydrate calculation, The purpose of this calculation is to answer the question, "Give the temperature and the composition if the gas, at what pressure will a hydrate form?" A similar calculation is to estimate the temperature at which the hydrate will form given pressure and the composition. The execution of these calculations is similar.

The objective functions to be solved are:

$$f_1(T) = 1 - \sum y_i / K_i \qquad (2\text{-}10)$$

$$f_2(P) = 1 - \sum y_i / K_i \qquad (2\text{-}11)$$

Depending on whether you want to calculate the pressure or the temperature, the appropriate function, either equation (2-5) or (2-6), is selected. Iterations are performed on the unknown variable until the summation is equal to unity. So to use the first equation (Equation 2-5), the pressure is known and iteration are performed on the temperature.

In chapter 3, the method used to carry out the project will be presented. The method include a primary study on general gas hydrate from available literature, hydrate temperature and pressure formation simulation using PetronasSim and hydrate equilibrium composition calculation using K-Factor method.

CHAPTER 3

METHODOLOGY

3.1 Primary Study on Clathrates

Clathrates is a new concept therefore in order to study the feasibility of utilizing their properties into separation of carbon dioxide from natural gas, they must be fully understood. Analysis of clathrates (composition, temperature and pressure formation, occurrence) in both nature and laboratory environment was carried out. Different equations of state were studied to see their applicability in the range of hydrate temperature and pressure formation. After that ranges of temperature, pressure, water/gas ratio, carbon dioxide level were chosen for the study based on general knowledge obtained.

3.2 Temperature and Pressure Formation Simulation

PetronasSim 2.55.2 was used as a software tool to obtain temperature and pressure in which hydrate formation. Gas and water composition as well as temperature are input and pressure are output. From the data obtained the graphs of pressure versus temperature were drawn at different gas composition as well as water/gas ratio. Pressure formation difference (at difference water/ gas ratio but at the same gas composition) versus temperature graph was also formed.

3.3 Hydrate Equilibrium Condition and Composition Calculation

K-factor method was use to calculate the equilibrium composition of gas hydrate. In K-factor method, water is assumed to be sufficient to form hydrate therefore composition was calculated on water free basis.

3.4 Equation of State

Peng-Robinson was chosen for the calculation of hydrate formation temperature and pressure due to it suitability with all fluid properties in natural gas.

```
                          ┌─────────┐
                          │  Start  │
                          └─────────┘
                               │
                               ▼
```

Open a stream of CO_2, CH_4, H_2O.

- In **Property Package**: Choose Advanced Peng-Robinson as thermodynamic model and Natural Gas Processing as Chemical System Categories.

- In **Components:** Add CO_2, CH_4, H_2O.

```
                               │
                               ▼
```

Open Hydrate calculation unit and connect it with the stream created above.

```
                               │
                               ▼
```

Input gas composition and water/gas ratio.

```
                               │
                               ▼
```

Compute CO_2, CH_4, H_2O fraction.(hand calculation)

```
                               │
                               ▼
```

Input CO_2, CH_4, H_2O fraction and designed temperature

```
                               │
                               ▼
```

Output hydrate pressure formation. (from PetronasSim)

```
                               │
                               ▼
                          ┌─────────┐
                          │   End   │
                          └─────────┘
```

Figure 3.1. Simulation steps to obtain temperature and pressure formation in PetronasSim.
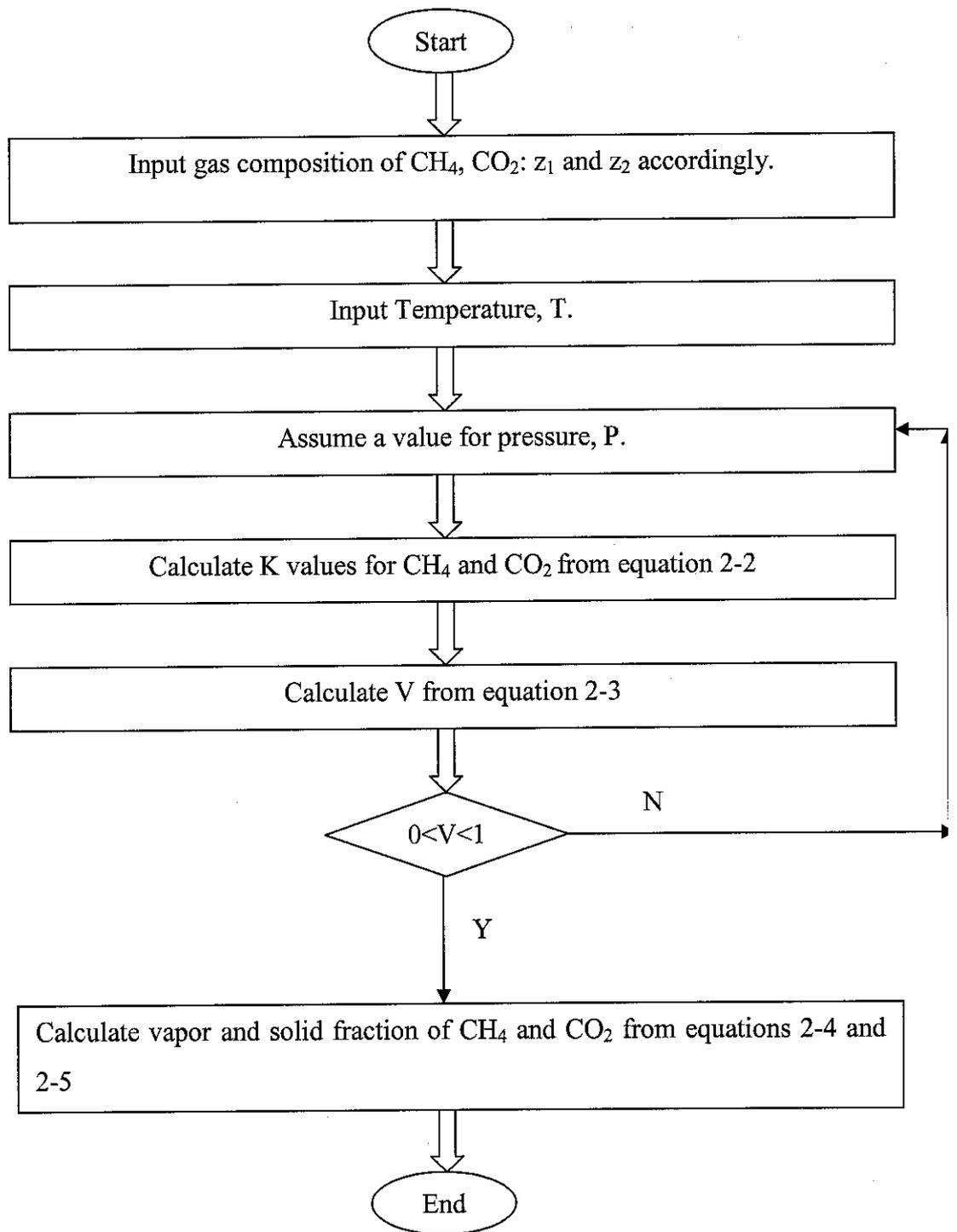
Figure 3.2. Calculation steps to obtain hydrate equilibrium composition using K-factor method.

3.5 Analysis

In hydrate equilibrium composition calculation using K-factor method, vapor phase fraction V indicates the fraction of gases in vapor form.. If vapor fraction calculated equals to 1 then that is the condition where hydrate phase start to form and temperature and pressure are formation T and P. If vapor phase equals to 0 then that is the condition where all gases form hydrate with water (actually there are still a small amount of gases are in equilibrium with hydrate). The pressure at which vapor phase equals to 0 is the highest pressure needed to convert almost all gases to hydrate in present of sufficient amount of water (water/gas ratio at least equals to 5.75). Above this pressure there is not much change in equilibrium composition. At one temperature and several range of pressure, equation 2-3 gives value of V in 0 to 1 range but only one range of pressure is correct since hydrate start to form one time then complete and are more stable as pressure increases. To make sure the pressure range use is correct it must be referred to PetronasSim result of temperature and pressure formation.

In chapter 4, the result of the above simulation will be presented and discussed in detail as follows:

1. Effect of temperature on pressure formation of CH_4 and CO_2 Hydrate
2. Effect of CO_2 content on pressure formation of CH_4 and CO_2 -mixture Hydrate
3. Effect of water/gas (w/g) ratio in feed on pressure formation of CH_4 and CO_2 Hydrate
4. Effect of pressure on hydrate phase equilibrium composition of CH_4 and CO_2 -mixture Hydrate
5. Effect of temperature on hydrate phase equilibrium composition of CH_4 and CO_2 -mixture hydrate

CHAPTER 4

RESULT and DISCUSSION

This section presents the data obtained from Simulation in PetronasSim and Computation using K-factor method. The discussion elaborates the effect of temperature, pressure, water/gas ratio, carbon dioxide content on hydrate formation condition as well as phase equilibrium composition. The data obtained is also compared to data from other sources. It should be noted that any trends and conclusions made in this discussion are based on the specific range of condition studied here. At different ranges of condition the behavior of hydrate formation could slightly change or totally different. The accuracy of data obtained and conclusion made is subjected to the accuracy of software and computation method used.

4.1 Effect of Temperature on Pressure Formation of CH_4 and CO_2 Hydrate

Figure 4.1 shows the plots of formation pressure of hydrate versus temperature at various CO_2 concentrations. These pressures data are obtained from PetronasSim by varying the temperature from -10 to 10 for different feed gas compositions (0, 10, 40, 60, 100 % CO_2). The positive slopes of the plots show that at higher the temperature, larger the pressure needed to form hydrate. Before the temperature of two degree Celsius the increase in formation pressure with respect to the increase in temperature is smaller as compared to that after two degree Celsius. This is observed from the slope of the P-T curve which is smaller before two degree Celsius then raise sharply after two degree Celsius. The change in slope of P-T curves can only be explained by the change in phase equilibrium. As the temperature is increased from negative to positive the phase equilibrium changes from I-H-V (Ice-Hydrate-Vapor) to L_w-H-V (Liquid water-Hydrate-Vapor). This change in phase equilibrium should occur at zero degree Celsius instead of two degree Celsius. With the current available data no firm conclusion can be drawn from this. Based on figure 2.5 (Makogon, 1997) the turning point (quadruple

point) should be at zero degree Celsius for P-T Hydrate formation curves of CH_4 and CO_2.
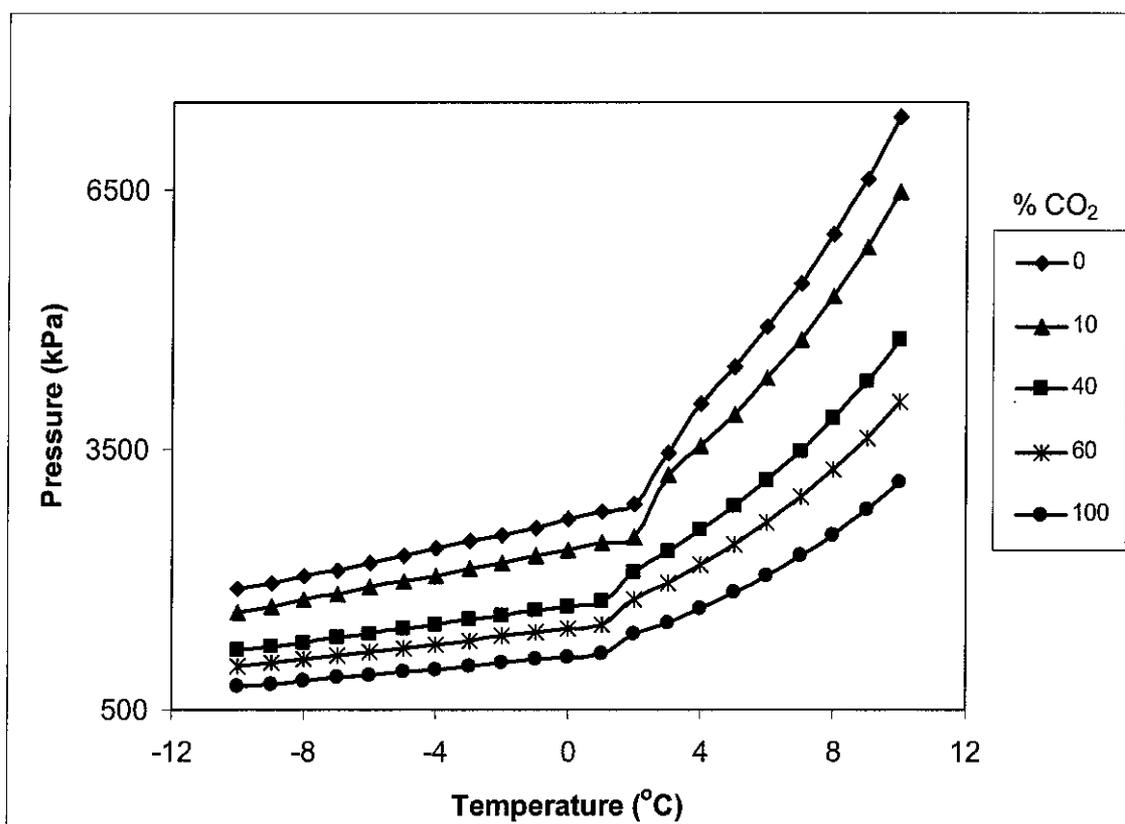
Figure 4.1: Pressure formation versus Temperature for Methane and Carbon Dioxide Hydrate at different Carbon Dioxide content (water/gas ratio equals to 5.75). (PetronasSim)

4.2 Effect of CO_2 content on Pressure formation of CH_4 and CO_2 -mixture Hydrate

Figure 4.1 shows the highest P-T curve is pure methane and the lowest curve is pure carbon dioxide. The P-T curve is lower as the carbon dioxide content of gas mixture increases which is represented by in creasing in percentage of carbon dioxide from 0%, 10% to 100%. This result shows that both gases CH_4 and CO_2 affect each other in term of hydrate formation. The present of CO_2 lower the hydrate formation pressure of CH_4

and the present of CH_4 elevate the hydrate formation pressure of CO_2 (at the same temperature).

4.3 Effect of Water/Gas (w/g) Ratio in Feed on Pressure Formation of CH_4 and CO_2 Hydrate

Figure 4.2 shows the hydrate-formation-pressure difference among various water/gas ratio feed. The pressures data are obtained from PetronasSim by varying the w/g ratio and temperature while keeping the composition of gas stream constant at 10% of CO_2. The w/g ratios studied are 1, 3, 5.75 and 7. The formation pressure at w/g ratio of 5.75 is taken as reference pressure (5.75 is the minimum w/g ratio of hydrate structure I where all cages are filled with gas molecules). Delta P for w/g ratio of 7 (greater than 5.75) is positive while delta P for w/g ratios of 1 and 3 (smaller than 5.75) are negative.
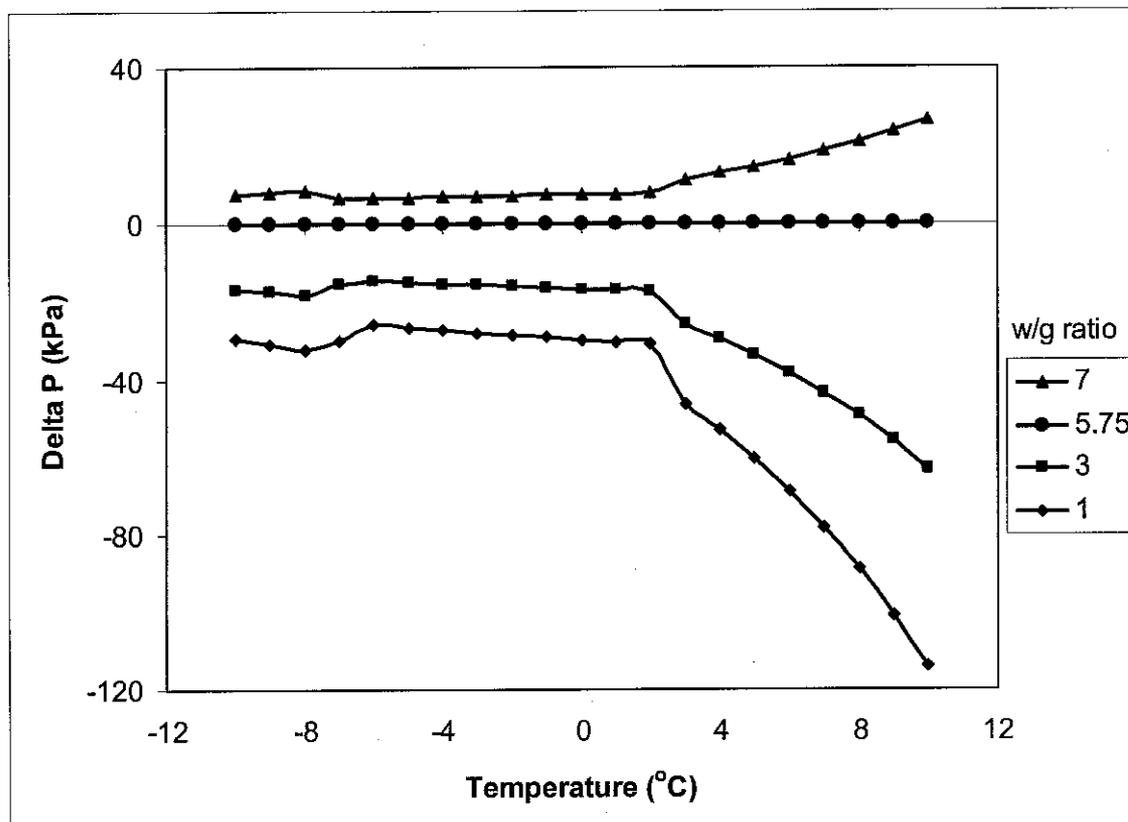
Figure 4.2: Delta P formation at various water/gas ratios to P formation at 5.75 water/gas ratio versus temperature (10% CO_2, 90% CH_4 gas stream). (PetronasSim)

30

This result indicates that the higher the w/g ratio in feed stream the more pressure needed to form hydrate. However the effect of w/g ratio on formation pressure is not much ranging from 0 to 3% (table 4.1). One interesting phenomenon is that pure methane or pure carbon dioxide pressure formation is not affected by w/g ratio.
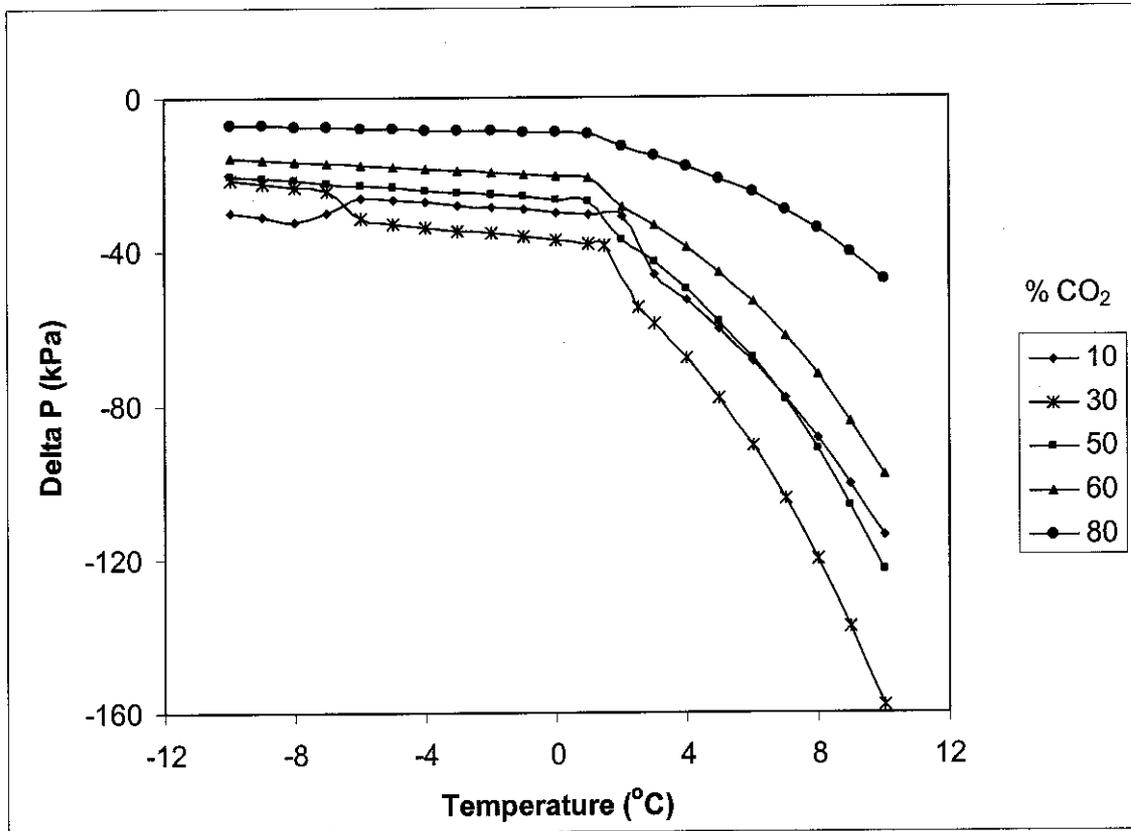
Figure 4.3: Delta P formation with respect to w/g ratio of 1 to 5.75 versus Temperature at different CO_2 gas content. (PetronasSim)

The graph above (Figure 4.3) is to compare the pressure formation at w/g ratio of 1 to the pressure formation at w/g ratio of 5.75 versus temperature for various CO_2 contents gas streams of 10%, 30%, 50%, and 80%. For example, the curve 10% represents the difference between formation pressure at w/g ratio of 1 and formation pressure at w/g ratio of 5.75 versus temperature for gas stream of 10% CO_2. All the Delta P curves are in negative region since at smaller water ratio (1<5.75) the required pressure for hydrate formation is lower as explained in the previous paragraph. When CO_2 content of gas stream is above 50% the change in formation pressure with respect to w/g ratio behaves

31

in more ordered manner. The higher the carbon dioxide content is, the less deviation in formation pressure with respect to change in w/g ratio is (80% curve is closer to x axis than 60% curve which in turn is closer to x axis as compared to 50% curve). In other words, for higher than 50% of CO_2 content gas stream, the higher the carbon dioxide content the less sensitive the formation pressure to w/g ratio. At 100% CO_2, the formation pressure is unaffected by change in w/g ratio. When content of gas stream is lower than 50% the change in formation pressure with respect to w/g ratio behaves in unpredictable manner with many up and down.

4.4 Effect of Pressure on Hydrate Phase Equilibrium Composition of CH₄ and CO_2 -mixture Hydrate

Figure 4.4 represents the phase impurity (%CO_2) versus pressure at 80% feed impurity and 0°C.
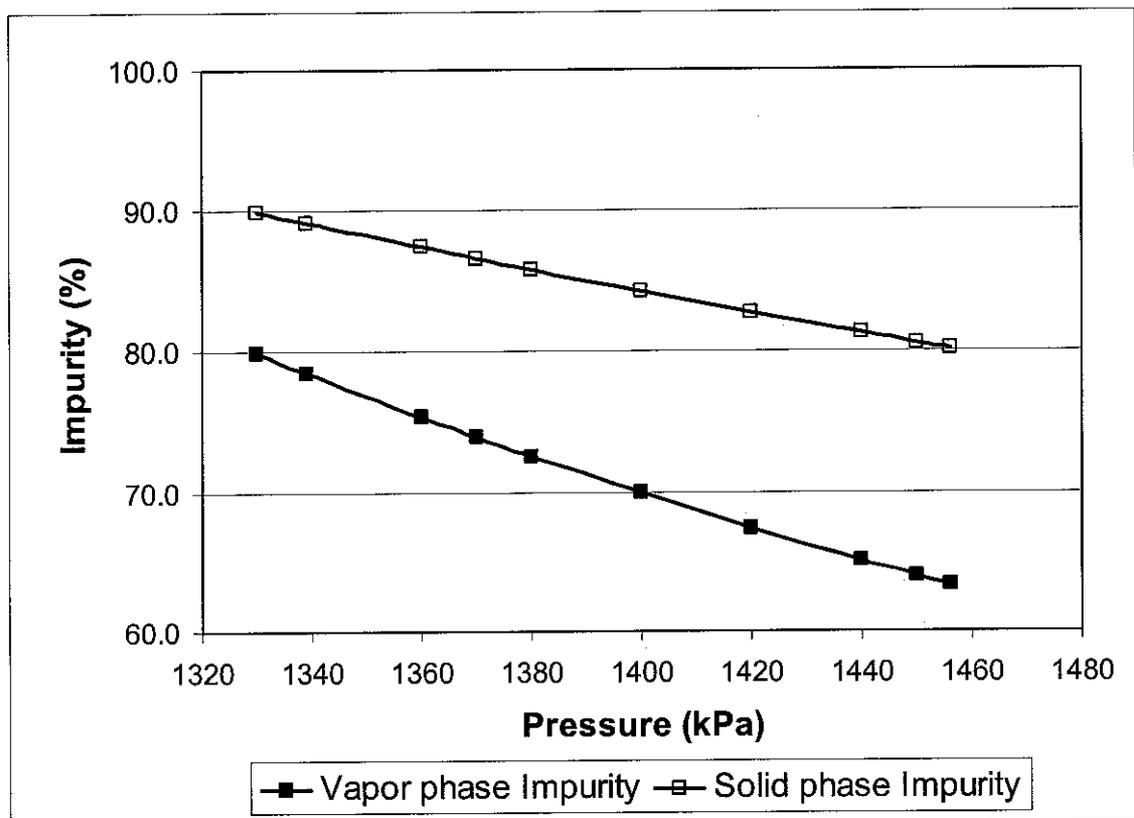
Figure 4.4: Phase impurity (%CO_2) versus pressure at 80% feed impurity and 0°C. (K-chart Method)

Phase compositions data are obtained by simulating a feed gas stream of 80% CO_2 and 20% CH_4 at temperature of 0°C and various pressures. Water is assumed to be sufficient to form hydrate. Formation pressure of hydrate at this composition of feed gas stream and temperature is 1329 kPa (the pressure that hydrate is just formed). Most of the gas is still in vapor form. Therefore vapor compositions of CO_2 and CH_4 are approximately 80%, 20% respectively while solid compositions are approximately 90% and 10% respectively.
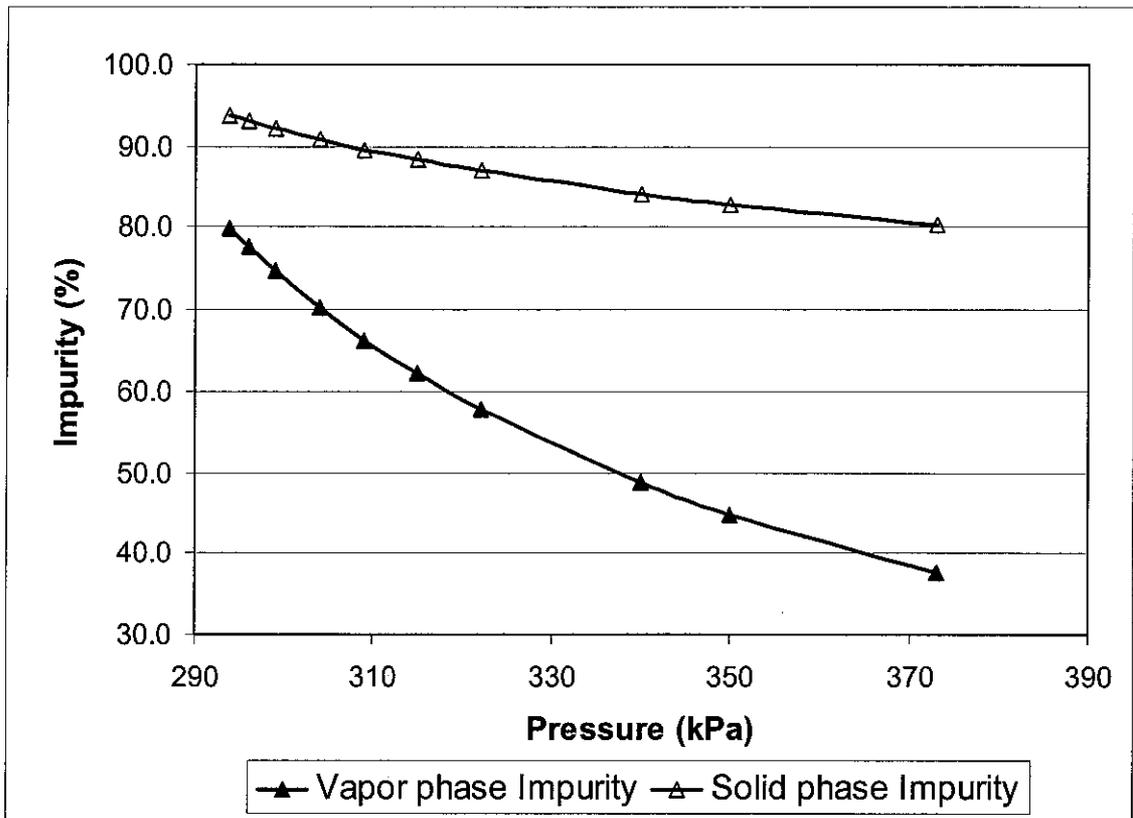
Figure 4.5: Phase impurity (%CO_2) versus pressure at 80% feed impurity and -6°C. (K-chart Method)

As the pressure increases, more hydrate forms which is indicated in reduction of vapor fraction (Table 4.1). Beside that both vapor and solid composition of CO_2 reduces as pressure increases which is indicated in the negative slope of both vapor phase impurity and solid phase impurity. This reduction of CO_2 in both vapor and solid phase is because as pressure increases, more CH_4 will be incorporated into hydrate lattice and

distributes itself into two phases. At pressure of 1457kPa almost all gases are incorporated in hydrate lattice. Therefore vapor compositions of CO_2 and CH_4 are approximately 63%, 27% respectively while solid compositions are approximately 80% and 20% respectively. Figure 4.5 and table 4.2 shows another data on phase composition versus pressure for 80% feed impurity calculated at -6 degree Celsius

Table 4.1: Phase compositions of CH_4 and CO_2 at $0^{o}C$ and various pressures (80% Feed Impurity). (K-chart method)

P (kPa)	Vapor fraction	Solid fraction	CO_2 vapor %	CH_4 vapor %	CO_2 solid %	CH_4 solid %
1330	0.98	0.02	79.8	20.2	89.9	10.1
1339	0.85	0.15	78.4	21.6	89.1	10.9
1360	0.61	0.39	75.3	24.7	87.4	12.6
1370	0.52	0.48	73.9	26.1	86.6	13.4
1380	0.44	0.56	72.6	27.4	85.8	14.2
1400	0.30	0.70	69.9	30.1	84.3	15.7
1420	0.18	0.82	67.5	32.5	82.8	17.2
1440	0.08	0.92	65.1	34.9	81.3	18.7
1450	0.03	0.97	64.0	36.0	80.6	19.4
1456	0.01	0.99	63.3	36.7	80.1	19.9

Table 4.2: Phase compositions of CH_4 and CO_2 at $-6^{o}C$ and various pressures (80% Feed Impurity). (K-chart method)

P (kPa)	Vapor fraction	Solid fraction	CO_2 vapor %	CH_4 vapor %	CO_2 solid %	CH_4 solid %
293.7	0.99	0.01	79.9	20.1	93.8	6.2
296	0.84	0.16	77.6	22.4	93.0	7.0
299	0.70	0.30	74.7	25.3	92.1	7.9
304	0.53	0.47	70.3	29.7	90.8	9.2
309	0.41	0.59	66.3	33.7	89.6	10.4
315	0.32	0.68	62.1	37.9	88.3	11.7
322	0.24	0.76	57.7	42.3	86.9	13.1
340	0.12	0.88	48.7	51.3	84.1	15.9
350	0.07	0.93	44.7	55.3	82.8	17.2
373	0.01	0.99	37.5	62.5	80.4	19.6

Figure 4.6 shows a combining phase impurity versus pressure curves at temperature of - 6, -3, 0, 10 ^{o}C. Pressure values do not present in the graph due to difference in hydrate

formation pressure range at different temperature. To see the exact Pressure values for phase impurity versus pressure curves at different temperature please refer to tables 4.1, 4.2, A3.13, and A3.14. Pressure increase according to pressure points from 1 to 10. From the data plotted, there's a similar behavior of change in gas composition at solid and vapor phases as pressure increases. When pressure increases, CO_2 composition in hydrate decreases. This indicates that at higher pressure selectivity of CO_2 to form hydrate decreases. This indicates that at higher pressure selectivity of CO_2 to form hydrate decreases why selectivity of CH_4 to form hydrate increases.
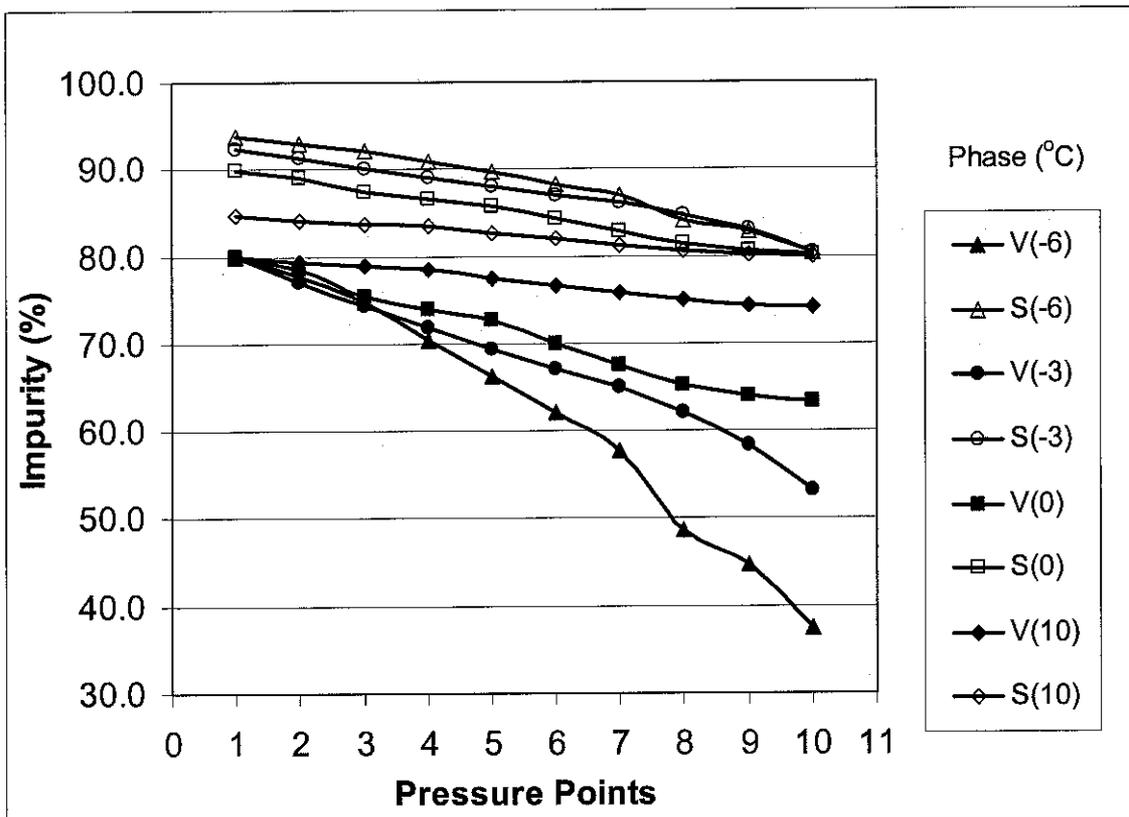
Figure 4.6: Phase impurity (%CO_2) versus temperature and pressure at 80% feed impurity. (K-chart Method)

4.5 Effect of Temperature on Hydrate Phase Equilibrium Composition of CH_4 and CO_2 -mixture Hydrate

From the graphs of phase impurity (%CO_2) versus temperature and pressure at 80% feed impurity (Figure 4.6), it is observed that all vapor curves start at CO_2 concentration

of 80%. That is the point where hydrate just starts to form; most of gases are in vapor form. All solid curves end at CO_2 concentration of 80% that is the point where most of gases form hydrate. At temperature of $-6^\circ C$ the Vapor and Solid curves are most far apart from each other and from the 80% CO_2 line. As the temperature increases the Vapor and Solids curves come closer to each other as well as to the 80% line. This indicates that as temperature increases the selectivity of CO_2 to form hydrate over CH_4 decreases. In term of separation of CO_2 and CH_4 into two phases, it is not favorable at high temperature but at low temperature. Figure 4.7 shows the plots of phase impurity versus pressure at various temperatures for feed gas impurity of 10%. For more graphs and tables of phase impurity (%CO_2) versus temperature and pressure at different feed impurity, please refer to appendices.
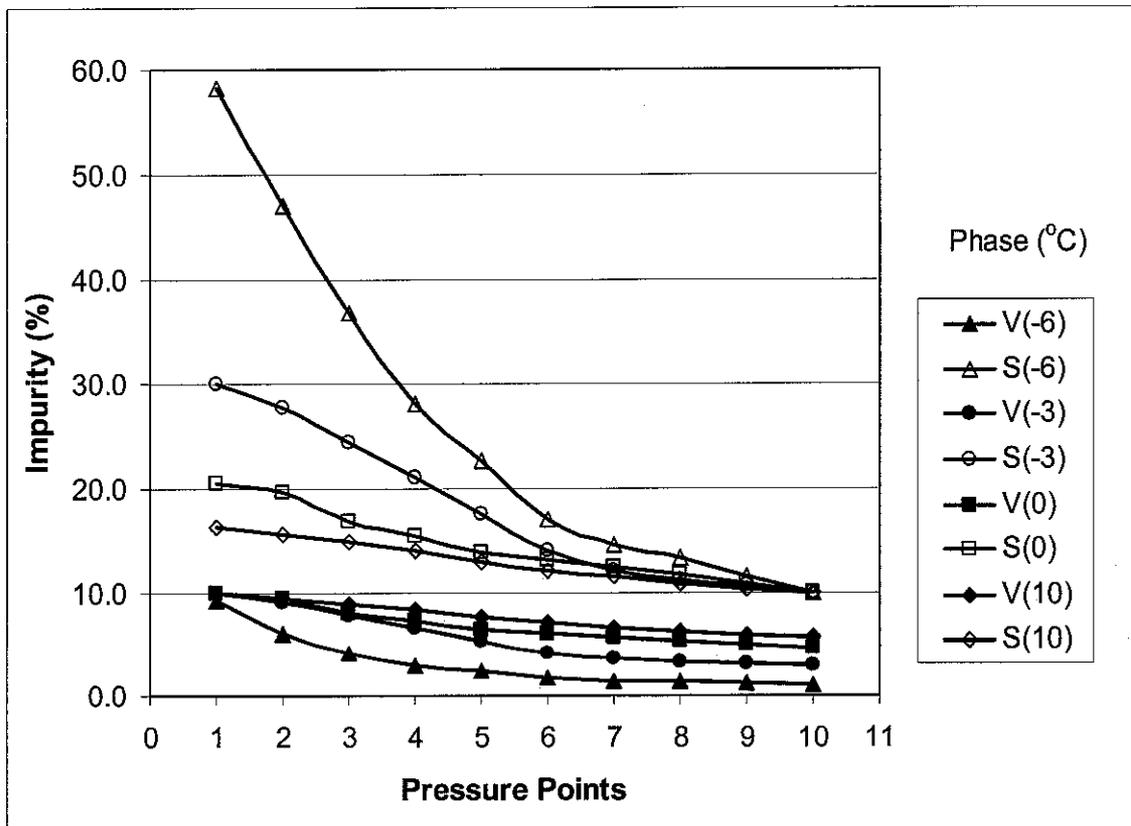
Figure 4.7: Phase impurity (%CO_2) versus temperature and pressure at 10% feed impurity. (K-chart Method)

CHAPTER 5

CONCLUSION

5.1 PetronasSim

PetronasSim is Petronas Steady State Simulator which is jointly developed by Petronas Research and Virtual Materials Group. PetronasSim version 2.55.2 used in this work is capable of predicting hydrate formation pressure (or formation temperature) at various temperature (or pressure), gas composition, water/gas ratio. Hydrate simulation in PetronasSim is built based on K-factor method and Advanced Peng-Robinson equation of state. PetronasSim is not capable of predicting the equilibrium composition of each phase when gas hydrate form. Hydrate formation pressure predicted by PetronasSim is slightly different from other literature.

5.2 K-factor method

K-factor method originated with Carson and Katz (1942). K-factor is defined as the distribution of the component between the hydrate and the gas which is available in literature for each of the components commonly encountered in natural gas. Calculation carried out using K-factor method in this work is based on water-free mole fraction basis. It is assumed that sufficient water is present to form hydrate. K factor method is able to give the phase equilibrium composition of gas hydrate when temperature and pressure are specified.

5.3 Trends observed

    a) Effect of temperature, pressure, carbon dioxide content, and water/gas ratio on hydrate formation of methane and carbon dioxide gas mixture.

As temperature increases formation pressure of gas hydrate increases and vice versa. Therefore to form gas hydrate at higher temperature requires more pressure. In I-H-V (Ice-Hydrate-Vapor) region, formation pressure increases as temperature increases less than in L_w-H-V (Liquid water-Hydrate-Vapor) region.

At the same temperature, the higher the carbon dioxide content of the gas, the lower the pressure required to form gas hydrate. Pure methane gas has highest formation pressures and pure carbon dioxide has lowest formation pressure as compared to methane-carbon dioxide gas mixtures at the same temperature. Both methane and carbon dioxide affect each other in term of hydrate formation.

At the same temperature and gas composition (carbon dioxide content), the higher the water/gas ratio (the more water present) the higher the pressure required to form gas hydrate. In this study a water/gas ratio of 1 gives lowest formation pressure and a water/gas ratio of 7 gives highest formation pressure. However a minimum water/gas ratio of 5.75 is required to convert all gases into hydrate. The increment in pressure needed to form hydrate when water content increases depend on the composition of gas mixture. The effect of water/gas ratio on hydrate formation is not as significant as temperature and pressure.

b) Effect of temperature and pressure on hydrate phase equilibrium composition.

At low temperature more carbon dioxide form hydrate as compared to methane. As temperature increases, the concentration of methane in hydrate increases. However the concentration of carbon dioxide in hydrate phase is always higher than that of vapor phase. The lower is the temperature the larger is the difference of concentration of carbon dioxide in hydrate phase and in vapor phase which indicates a better separation.

At low pressure region (associated with low temperature) the higher the pressure the lower the concentration of carbon dioxide in vapor phase or the more carbon dioxide form hydrate. However increase in pressure cause vapor phase to reduces since gases are incorporated in hydrate lattice more.

Lastly, PetronasSim and K-factor method are only considered as means for prediction of hydrate formation temperature, pressure, phase's equilibrium composition. They give the trends and effect of temperature, pressure, gas composition, water content to the formation of gas hydrate. The exact temperature, pressure, phase's equilibrium composition must be determined from experiment.

CHAPTER 6

RECOMMENDATION

This study has shown a positive result in the theoretical possibility of separating carbon dioxide from methane (or purifying methane gas) by using gas hydration. The hydrate formation temperature and pressure, phase equilibrium composition obtained through this study should be used only as reference for experiment study. The exact values should be obtained from experimental work. The suggested next steps would be:

a) Study on how to carry out experiments to obtain true values of hydrate formation temperature and pressure, and phase equilibrium composition of methane and carbon dioxide hydrate

This step is important to determine the exact range of temperature and pressure that is feasible for separation of carbon dioxide from methane. In natural gas, there are other gases such as ethane, propane, butane, nitrogen...which also affect the formation temperature and pressure of hydrate.

b) Study on the kinetic formation of gas hydrate.

This step is to determine how long the system reaches equilibrium state as well as factors affecting the rate of formation of hydrate. This information is necessary in determining the size of equipment needed for separation process as well as materials flow rate.

c) Study on heat of formation, heat capacity, and thermal conductivity of hydrates.

This step is important to provide data for determining the heat flow in and out of the system. Consequently it provides information for designing heating or cooling utilities of the process.

d) Study on separation equipments

This step is to design a system of equipments which is able cope the following conditions:

- Low temperature and high pressure operating conditions.
- Solid hydrate will stick to the wall of equipment when it is formed.
- Separating equilibrium vapor and solid phases.
- Hydrate dissociation results in dangerous pressure hazard in confined space.
- Recycle stream to gain higher recovery of methane.
- Changing in operating temperature and pressure (or a series of equipments which operate at different temperature and pressure) according to carbon dioxide content of feed gas to obtain optimum separation.

This hydration process could be suggested for pre-purification of high carbon dioxide content natural gas as well. The process and equipment used for pre-purification should be less complicated than that of purification process.

APPENDIX 1

No.	Detail/ Week	1	2	3	4	5	6	7	8	9	10	11	12	13	14	20
1	Selection of Project Topic	■														
2	Preliminary research work		■	■	■											
3	Submission of Preliminary report				x											
4	Project Work				■	■	■	■	■	■	■	■				
	Familiarization with Hysis				■											
	Tools research					■	■	■	■	■						
*	Submission of Progress report								x							
	Familiarization with PetronasSim									■						
	Effect of temperature, pressure, w/g study										■	■	■			
	Phase equilibrium composition study											■	■	■		
5	Submission of Dissertation Final Draft													x		
6	Submission of project Dissertation														x	
7	Oral Presentation															x

Table A1: Gantt chart

43

APPENDIX 2

Table A2: Geological parameters and Gas content within Artic region.

Geological Parameters and Gas Content Within Arctic Regions							
Region	Geo-thermal Gradient Degrees C/100m	Formation Pore Pressures	Gas Content	Pore Water salinities (ppt)	Gas Hydrate Stability Zone (depth to base)	Occur-rence	Potential Volume (cubic meters m^3)
Northern Alaska	1.5° Prudhoe Bay 4.5° NPRA	Normal 9.795kPa/m; 0.433psi/ft	87-99% methane	0.15-0.50 permafrost 0.50-19.0 below permafrost	>1000 m	Multiple zones 3-31m thick; free gas; stratigraphic accumulation	$10x10^{12}$ - $12x10^{12}$
McKenzie Delta Beaufort Sea	3.0°-4.0° beneath permafrost	Beneath permafrost offshore - abnormally high; onshore normal 9.795kPa/m; 0.433psi/ft	99.19-99.53% methane	5-35	200-1200 m max 1200m Richards Island	Mallik Field Sandstones and conglomerates depth 820-1.103m, 40-250m thick; Outer McKenzie Delta depth 330-335m thin ice layers	$9.3x10^{12}$ - $2.7x10^{12}$ McKenzie Delta
Sverdrup Basin, Canada	Offshore 1.3°-2.5° Onshore: permafrost 4.0-8.0; below permafrost 3.0-6.0	Normal	Methane	Not Available	36-1138m	King Christian 160m Ellef inges 2560m Melville Islands 356-895m	Not Available
Western Siberia Basin, Russia	2.0-5.0	Normal	Methane	5-14 below permafrost	0-1000m	Depth 720-820m; upper 40 m of reservoir. Lower free gas	$80x10^9$ 30% in upper permafrost.
Lena-Tunguska, Russia	2.0 Vilyuy Basin	Under-pressured 1.3-3.0Mpa. Lower than hydrostatic	Methane	1-10	2000m 800-1000m Vilyuy Basin		Potential volume-not available; gas flows 120,000m^3/d
Timan-Pechora Basin, Russia	1.0-3.0	Under-pressured 1.8MPa	Methane	Low salinities	600-800 m	Small amounts of gas associated with coals in near surface Cretaceous may indicate gas hydrates	Very little in post-Permian rocks
Northeastern Siberia and Kamchatka, Russia					500-1000 m	Frontier area; northwestern areas show best potential	
Svalbard Archipelago, Norway					100-460 m	Frontier area	Significant shallow gas flows during drilling in permafrost and sub-permafrost sections

APPENDIX 3

Table A3.1: Hydrate temperature and pressure formation. (PetronasSim)

	T (C)	P (kPa)		T (C)	P (kPa)		T (C)	P (kPa)
$CO_2\%$ 0 $CH_4\%$ 100 water/gas 5.75	-10	1901.51	$CO_2\%$ 5 $CH_4\%$ 95 water/gas 5.75	-10	1769.74	$CO_2\%$ 10 $CH_4\%$ 90 water/gas 5.75	-10	1629.5
	-9	1974.84		-9	1838.27		-9	1702.71
	-8	2049.65		-8	1908.2		-8	1777.96
	-7	2125.92		-7	1979.5		-7	1851.56
	-6	2203.6		-6	2052.14		-6	1919.78
	-5	2282.66		-5	2126.09		-5	1989.25
	-4	2363.06		-4	2201.32		-4	2059.92
	-3	2444.76		-3	2277.77		-3	2131.76
	-2	2527.72		-2	2355.41		-2	2204.73
	-1	2611.88		-1	2434.19		-1	2278.79
	0	2697.19		0	2514.07		0	2353.9
	1	2783.6		1	2594.99		1	2430
	2	2871.05		2	2676.91		2	2507.04
	3	3471.17		3	3420.46		3	3205.59
	4	4041.4		4	3774.36		4	3539.24
	5	4457.07		5	4165.44		5	3908.21
	6	4916.77		6	4598.31		6	4316.87
	7	5426.09		7	5078.29		7	4770.37
	8	5991.52		8	5611.67		8	5274.74
	9	6620.71		9	6205.8		9	5837.12
	10	7322.66		10	6869.44		10	6466

Table A3.2: Hydrate temperature and pressure formation. (PetronasSim)

	T (C)	P (kPa)		T (C)	P (kPa)		T (C)	P (kPa)
$CO_2\%$ 20 $CH_4\%$ 80 water/gas 5.75	-10	1416.28	$CO_2\%$ 30 $CH_4\%$ 70 water/gas 5.75	-10	1286.81	$CO_2\%$ 40 $CH_4\%$ 60 water/gas 5.75	-10	1190.85
	-9	1479.63		-9	1344.21		-9	1238.02
	-8	1544.72		-8	1403.21		-8	1286.21
	-7	1611.53		-7	1463.74		-7	1335.39
	-6	1680.06		-6	1525.81		-6	1385.54
	-5	1750.28		-5	1582.37		-5	1436.65
	-4	1822.19		-4	1639.37		-4	1488.68
	-3	1889.55		-3	1697.35		-3	1541.62
	-2	1954.72		-2	1756.27		-2	1595.43
	-1	2020.89		-1	1816.1		-1	1650.09
	0	2088.01		0	1876.82		0	1705.56
	1	2156.03		1	1938.37		1	1761.81
	2	2224.93		2	2138.52		2	2104.21
	3	2846.91		3	2560.36		3	2327.02
	4	3145.85		4	2830.72		4	2573.59
	5	3476.76		5	3130.24		5	2846.89
	6	3843.71		6	3462.65		6	3150.39
	7	4251.45		7	3832.38		7	3488.21
	8	4705.59		8	4244.68		8	3865.29
	9	5212.83		9	4705.86		9	4287.59
	10	5781.24		10	5223.59		10	4762.42

	T (C)	P (kPa)		T (C)	P (kPa)		T (C)	P (kPa)
	-10	1090.27		-10	1006.09		-10	934.66
CO₂%	-9	1133.67	CO₂%	-9	1046.31	CO₂%	-9	972.15
50	-8	1178	60	-8	1087.4	70	-8	1010.47
CH₄%	-7	1223.26	CH₄%	-7	1129.35	CH₄%	-7	1049.6
50	-6	1269.42	40	-6	1172.14	30	-6	1089.52
water/gas	-5	1316.47	water/gas	-5	1215.77	water/gas	-5	1130.21
5.75	-4	1364.38	5.75	-4	1260.19	5.75	-4	1171.66
	-3	1413.12		-3	1305.41		-3	1213.85
	-2	1462.69		-2	1351.38		-2	1256.75
	-1	1513.04		-1	1398.09		-1	1300.34
	0	1564.14		0	1445.5		0	1344.6
	1	1615.97		1	1493.59		1	1389.49
	2	1929.09		2	1782.05		2	1656.93
	3	2133.74		3	1971.27		3	1832.88
	4	2360.27		4	2180.73		4	2027.66
	5	2611.43		5	2412.99		5	2243.65
	6	2890.46		6	2671.1		6	2483.68
	7	3201.22		7	2958.66		7	2751.18
	8	3548.34		8	3280.05		8	3050.28
	9	3937.48		9	3640.66		9	3386.12
	10	4375.65		10	4047.21		10	3765.19

Table A3.3: Hydrate temperature and pressure formation. (PetronasSim)

	T (C)	P (kPa)		T (C)	P (kPa)
	-10	873.31		-10	773.4
CO₂%	-9	908.46	CO₂%	-9	804.71
80	-8	944.39	100	-8	836.72
CH₄%	-7	981.08	CH₄%	-7	869.4
20	-6	1018.51	0	-6	902.76
water/gas	-5	1056.68	water/gas	-5	936.78
5.75	-4	1095.56	5.75	-4	971.43
	-3	1135.13		-3	1006.71
	-2	1175.38		-2	1042.59
	-1	1216.27		-1	1079.05
	0	1257.79		0	1116.07
	1	1299.91		1	1153.63
	2	1549.25		2	1373.46
	3	1713.72		3	1519.05
	4	1895.75		4	1680.1
	5	2097.59		5	1858.61
	6	2321.9		6	2056.94
	7	2571.91		7	2277.98
	8	2851.54		8	2525.33
	9	3165.72		9	2803.56
	10	3520.75		10	3118.71

Table A3.4: Hydrate temperature and pressure formation. (PetronasSim)

Table A3.5: Hydrate Pressure formation at different Water/Gas ratios. (PetronasSim)					
T (C)		P1 (kPa)		P2 (kPa)	Delta (P2-P1)	% Change
-10		1629.5		1599.79	-29.71	1.82
-9	water/gas	1702.71	water/gas	1671.75	-30.96	1.82
-8	5.75	1777.96	1	1745.72	-32.24	1.81
-7	CO2%	1851.56	CO2%	1821.69	-29.87	1.61
-6	10	1919.78	10	1893.83	-25.95	1.35
-5	CH4%	1989.25	CH4%	1962.65	-26.6	1.34
-4	90	2059.92	90	2032.68	-27.24	1.32
-3		2131.76		2103.88	-27.88	1.31
-2		2204.73		2176.21	-28.52	1.29
-1		2278.79		2249.64	-29.15	1.28
0		2353.9		2324.11	-29.79	1.27
1		2430		2399.58	-30.42	1.25
2		2507.04		2476	-31.04	1.24
3		3205.59		3159.38	-46.21	1.44
4		3539.24		3486.44	-52.8	1.49
5		3908.21		3847.95	-60.26	1.54
6		4316.87		4248.2	-68.67	1.59
7		4770.37		4692.23	-78.14	1.64
8		5274.74		5185.96	-88.78	1.68
9		5837.12		5736.41	-100.71	1.73
10		6466		6351.99	-114.01	1.76

Table A3.6: Hydrate Pressure formation at different Water/Gas ratios. (PetronasSim)					
T (C)		P1 (kPa)		P2 (kPa)	Delta (P2-P1)	% Change
-10		1629.5		1612.65	-16.85	1.03
-9	water/gas	1702.71	water/gas	1685.15	-17.56	1.03
-8	5.75	1777.96	3	1759.68	-18.28	1.03
-7	CO2%	1851.56	CO2%	1836.21	-15.35	0.83
-6	10	1919.78	10	1905.22	-14.56	0.76
-5	CH4%	1989.25	CH4%	1974.32	-14.93	0.75
-4	90	2059.92	90	2044.63	-15.29	0.74
-3		2131.76		2116.11	-15.65	0.73
-2		2204.73		2188.72	-16.01	0.73
-1		2278.79		2262.42	-16.37	0.72
0		2353.9		2337.17	-16.73	0.71
1		2430		2412.91	-17.09	0.70
2		2507.04		2489.6	-17.44	0.70
3		3205.59		3179.75	-25.84	0.81
4		3539.24		3509.77	-29.47	0.83
5		3908.21		3874.63	-33.58	0.86
6		4316.87		4278.67	-38.2	0.88
7		4770.37		4726.97	-43.4	0.91
8		5274.74		5225.52	-49.22	0.93
9		5837.12		5781.38	-55.74	0.95
10		6466		6403.01	-62.99	0.97

Table A3.7: Hydrate Pressure formation at different Water/Gas ratios. (PetronasSim)					
T (C)		P1 (kPa)		P2 (kPa)	Delta (P2-P1)	% Change

T (C)		P1 (kPa)		P2 (kPa)	Delta (P2-P1)	% Change
-10		1629.5		1637	7.5	0.46
-9	water/gas	1702.71	water/gas	1710.53	7.82	0.46
-8	5.75	1777.96	7	1786.1	8.14	0.46
-7	CO2%	1851.56	CO2%	1857.75	6.19	0.33
-6	10	1919.78	10	1926.14	6.36	0.33
-5	CH4%	1989.25	CH4%	1995.77	6.52	0.33
-4	90	2059.92	90	2066.6	6.68	0.32
-3		2131.76		2138.6	6.84	0.32
-2		2204.73		2211.74	7.01	0.32
-1		2278.79		2285.96	7.17	0.31
0		2353.9		2361.22	7.32	0.31
1		2430		2437.48	7.48	0.31
2		2507.04		2514.69	7.65	0.31
3		3205.59		3216.78	11.19	0.35
4		3539.24		3551.96	12.72	0.36
5		3908.21		3922.64	14.43	0.37
6		4316.87		4333.23	16.36	0.38
7		4770.37		4788.89	18.52	0.39
8		5274.74		5295.66	20.92	0.40
9		5837.12		5860.72	23.6	0.40
10		6466		6492.58	26.58	0.41

Table A3.8: Hydrate Pressure formation at different Water/Gas ratios. (PetronasSim)					
T (C)		P1 (kPa)		P2 (kPa)	Delta (P2-P1)	% Change

T (C)		P1 (kPa)		P2 (kPa)	Delta (P2-P1)	% Change
-10		1286.81		1265.32	-21.49	1.67
-9	water/gas	1344.21	water/gas	1321.87	-22.34	1.66
-8	5.75	1403.21	1	1379.96	-23.25	1.66
-7	CO2%	1463.74	CO2%	1439.57	-24.17	1.65
-6	30	1525.81	30	1494.41	-31.4	2.06
-5	CH4%	1582.37	CH4%	1549.57	-32.8	2.07
-4	70	1639.37	70	1605.73	-33.64	2.05
-3		1697.35		1662.86	-34.49	2.03
-2		1756.27		1720.94	-35.33	2.01
-1		1816.1		1779.94	-36.16	1.99
0		1876.82		1839.81	-37.01	1.97
1		1938.37		1900.52	-37.85	1.95
1.5		1969.44		1931.18	-38.26	1.94
2.5		2435.09		2380.31	-54.78	2.25
3		2560.36		2501.46	-58.9	2.30
4		2830.72		2762.68	-68.04	2.40
5		3130.24		3051.71	-78.53	2.51
6		3462.65		3372.12	-90.53	2.61
7		3832.38		3728.12	-104.26	2.72
8		4244.68		4124.74	-119.94	2.83
9		4705.86		4568.07	-137.79	2.93
10		5223.59		5065.55	-158.04	3.03

		Table A3.9: Hydrate Pressure formation at different Water/Gas ratios. (PetronasSim)				
T (C)			**P1 (kPa)**	**P2 (kPa)**	**Delta (P2-P1)**	**% Change**
-10			1090.27	1069.98	-20.29	1.86
-9	water/gas		1133.67	1112.77	-20.9	1.84
-8		5.75	1178	1156.5	-21.5	1.83
-7	CO2%		1223.26	1201.14	-22.12	1.81
-6		50	1269.42	1246.69	-22.73	1.79
-5	CH4%		1316.47	1293.12	-23.35	1.77
-4		50	1364.38	1340.4	-23.98	1.76
-3			1413.12	1388.53	-24.59	1.74
-2			1462.69	1437.46	-25.23	1.72
-1			1513.04	1487.18	-25.86	1.71
0			1564.14	1537.66	-26.48	1.69
1			1615.97	1588.86	-27.11	1.68
2			1929.09	1892.25	-36.84	1.91
3			2133.74	2090.81	-42.93	2.01
4			2360.27	2310.27	-50	2.12
5			2611.43	2553.23	-58.2	2.23
6			2890.46	2822.76	-67.7	2.34
7			3201.22	3122.51	-78.71	2.46
8			3548.34	3456.89	-91.45	2.58
9			3937.48	3831.32	-106.16	2.70
10			4375.65	4252.56	-123.09	2.81

		Table A3.10: Hydrate Pressure formation at different Water/Gas ratios. (PetronasSim)				
T (C)			**P1 (kPa)**	**P2 (kPa)**	**Delta (P2-P1)**	**% Change**
-10			1090.27	1069.98	-20.29	1.86
-9	water/gas		1133.67	1112.77	-20.9	1.84
-8		5.75	1178	1156.5	-21.5	1.83
-7	CO2%		1223.26	1201.14	-22.12	1.81
-6		50	1269.42	1246.69	-22.73	1.79
-5	CH4%		1316.47	1293.12	-23.35	1.77
-4		50	1364.38	1340.4	-23.98	1.76
-3			1413.12	1388.53	-24.59	1.74
-2			1462.69	1437.46	-25.23	1.72
-1			1513.04	1487.18	-25.86	1.71
0			1564.14	1537.66	-26.48	1.69
1			1615.97	1588.86	-27.11	1.68
2			1929.09	1892.25	-36.84	1.91
3			2133.74	2090.81	-42.93	2.01
4			2360.27	2310.27	-50	2.12
5			2611.43	2553.23	-58.2	2.23
6			2890.46	2822.76	-67.7	2.34
7			3201.22	3122.51	-78.71	2.46
8			3548.34	3456.89	-91.45	2.58
9			3937.48	3831.32	-106.16	2.70
10			4375.65	4252.56	-123.09	2.81

T (C)		P1 (kPa)		P2 (kPa)	Delta (P2-P1)	% Change
Table A3.11: Hydrate Pressure formation at different Water/Gas ratios. (PetronasSim)						
-10		1006.09		990.54	-15.55	1.55
-9	water/gas	1046.31	water/gas	1030.28	-16.03	1.53
-8	5.75	1087.4	7	1070.89	-16.51	1.52
-7	CO2%	1129.35	CO2%	1112.37	-16.98	1.50
-6	60	1172.14	60	1154.68	-17.46	1.49
-5	CH4%	1215.77	CH4%	1197.82	-17.95	1.48
-4	40	1260.19	40	1241.76	-18.43	1.46
-3		1305.41		1286.48	-18.93	1.45
-2		1351.38		1331.97	-19.41	1.44
-1		1398.09		1378.18	-19.91	1.42
0		1445.5		1425.11	-20.39	1.41
1		1493.59		1472.71	-20.88	1.40
2		1782.05		1753.55	-28.5	1.60
3		1971.27		1937.94	-33.33	1.69
4		2180.73		2141.78	-38.95	1.79
5		2412.99		2367.5	-45.49	1.89
6		2671.1		2617.97	-53.13	1.99
7		2958.66		2896.63	-62.03	2.10
8		3280.05		3207.66	-72.39	2.21
9		3640.66		3556.23	-84.43	2.32
10		4047.21		3948.84	-98.37	2.43

T (C)		P1 (kPa)		P2 (kPa)	Delta (P2-P1)	% Change
Table A3.12: Hydrate Pressure formation at different Water/Gas ratios. (PetronasSim)						
-10		873.31		866.32	-6.99	0.80
-9	water/gas	908.46	water/gas	901.26	-7.2	0.79
-8	5.75	944.39	7	936.97	-7.42	0.79
-7	CO2%	981.08	CO2%	973.44	-7.64	0.78
-6	80	1018.51	80	1010.65	-7.86	0.77
-5	CH4%	1056.68	CH4%	1048.59	-8.09	0.77
-4	20	1095.56	20	1087.25	-8.31	0.76
-3		1135.13		1126.59	-8.54	0.75
-2		1175.38		1166.61	-8.77	0.75
-1		1216.27		1207.28	-8.99	0.74
0		1257.79		1248.57	-9.22	0.73
1		1299.91		1290.46	-9.45	0.73
2		1549.25		1536.26	-12.99	0.84
3		1713.72		1698.44	-15.28	0.89
4		1895.75		1877.79	-17.96	0.95
5		2097.59		2076.46	-21.13	1.01
6		2321.9		2297.05	-24.85	1.07
7		2571.91		2542.67	-29.24	1.14
8		2851.54		2817.13	-34.41	1.21
9		3165.72		3125.22	-40.5	1.28
10		3520.75		3473.1	-47.65	1.35

Table A3.13: Phase compositions of CH_4 and CO_2 at -3°C and various pressures (80% Feed Impurity). (K-chart method)

P (kPa)	Vapor fraction	Solid fraction	CO_2 vapor %	CH_4 vapor %	CO_2 solid %	CH_4 solid %
725	0.99	0.01	79.9	20.1	92.4	7.6
735	0.79	0.21	77.0	23.0	91.2	8.8
745	0.64	0.36	74.3	25.7	90.1	9.9
755	0.52	0.48	71.8	28.2	89.1	10.9
765	0.43	0.57	69.4	30.6	88.0	12.0
775	0.35	0.65	67.2	32.8	87.0	13.0
785	0.29	0.71	65.0	35.0	86.1	13.9
800	0.21	0.79	62.1	37.9	84.7	15.3
820	0.12	0.88	58.5	41.5	83.0	17.0
853	0.01	0.99	53.3	46.7	80.3	19.7

Table A3.14: Phase compositions of CH_4 and CO_2 at 10°C and various pressures (80% Feed Impurity). (K-chart method)

P (kPa)	Vapor fraction	Solid fraction	CO_2 vapor %	CH_4 vapor %	CO_2 solid %	CH_4 solid %
4438	0.99	0.01	79.9	20.1	84.6	15.4
4445	0.85	0.15	79.3	20.7	84.1	15.9
4450	0.76	0.24	78.8	21.2	83.7	16.3
4455	0.68	0.32	78.4	21.6	83.4	16.6
4465	0.51	0.49	77.5	22.5	82.7	17.3
4475	0.36	0.64	76.6	23.4	81.9	18.1
4485	0.23	0.77	75.7	24.3	81.2	18.8
4495	0.10	0.90	74.8	25.2	80.5	19.5
4500	0.04	0.96	74.4	25.6	80.2	19.8
4502	0.01	0.99	74.2	25.8	80.1	19.9

Table A3.15: Phase compositions of CH_4 and CO_2 at -6°C and various pressures (60% Feed Impurity). (K-chart method)

P (kPa)	Vapor fraction	Solid fraction	CO_2 vapor %	CH_4 vapor %	CO_2 solid %	CH_4 solid %
319	0.98	0.02	59.5	40.5	87.5	12.5
325	0.87	0.13	56.0	44.0	86.4	13.6
330	0.79	0.21	53.4	46.6	85.6	14.4
340	0.68	0.32	48.7	51.3	84.1	15.9
360	0.54	0.46	41.3	58.7	81.7	18.3
380	0.45	0.55	35.7	64.3	79.7	20.3
410	0.36	0.64	29.5	70.5	77.3	22.7
460	0.27	0.73	22.7	77.3	74.0	26.0
580	0.13	0.87	14.2	85.8	67.1	32.9
690	0.01	0.99	10.2	89.8	60.5	39.5

Table A3.16: Phase compositions of CH_4 and CO_2 at -3°C and various pressures (60% Feed Impurity). (K-chart method)

P (kPa)	Vapor fraction	Solid fraction	CO_2 vapor %	CH_4 vapor %	CO_2 solid %	CH_4 solid %
812	0.99	0.01	59.9	40.1	83.7	16.3
825	0.90	0.10	57.6	42.4	82.5	17.5
840	0.82	0.18	55.2	44.8	81.3	18.7
860	0.72	0.28	52.3	47.7	79.7	20.3
900	0.56	0.44	47.1	52.9	76.7	23.3
940	0.45	0.55	42.7	57.3	73.9	26.1
980	0.35	0.65	39.0	61.0	71.2	28.8
1020	0.26	0.74	35.7	64.3	68.6	31.4
1090	0.13	0.87	30.8	69.2	64.2	35.8
1150	0.01	0.99	27.3	72.7	60.4	39.6

Table A3.17: Phase compositions of CH_4 and CO_2 at $0^{\circ}C$ and various pressures (60% Feed Impurity). (K-chart method)

P (kPa)	Vapor fraction	Solid fraction	CO_2 vapor %	CH_4 vapor %	CO_2 solid %	CH_4 solid %
1490	0.99	0.01	59.7	40.3	77.8	22.2
1520	0.83	0.17	56.8	43.2	75.7	24.3
1550	0.70	0.30	54.1	45.9	73.8	26.2
1580	0.58	0.42	51.5	48.5	71.8	28.2
1610	0.48	0.52	49.1	50.9	69.9	30.1
1640	0.38	0.62	46.8	53.2	68.0	32.0
1670	0.29	0.71	44.6	55.4	66.2	33.8
1700	0.20	0.80	42.6	57.4	64.4	35.6
1730	0.12	0.88	40.6	59.4	62.5	37.5
1770	0.01	0.99	38.2	61.8	60.1	39.9

Table A3.18: Phase compositions of CH_4 and CO_2 at $10^{\circ}C$ and various pressures (60% Feed Impurity). (K-chart method)

P (kPa)	Vapor fraction	Solid fraction	CO_2 vapor %	CH_4 vapor %	CO_2 solid %	CH_4 solid %
4690	0.99	0.01	59.9	40.1	68.2	31.8
4705	0.87	0.13	58.9	41.1	67.3	32.7
4720	0.76	0.24	57.9	42.1	66.5	33.5
4735	0.65	0.35	57.0	43.0	65.7	34.3
4755	0.51	0.49	55.7	44.3	64.5	35.5
4775	0.38	0.62	54.5	45.5	63.5	36.5
4795	0.26	0.74	53.2	46.8	62.4	37.6
4810	0.17	0.83	52.4	47.6	61.6	38.4
4825	0.09	0.91	51.5	48.5	60.8	39.2
4840	0.01	0.99	50.6	49.4	60.1	39.9
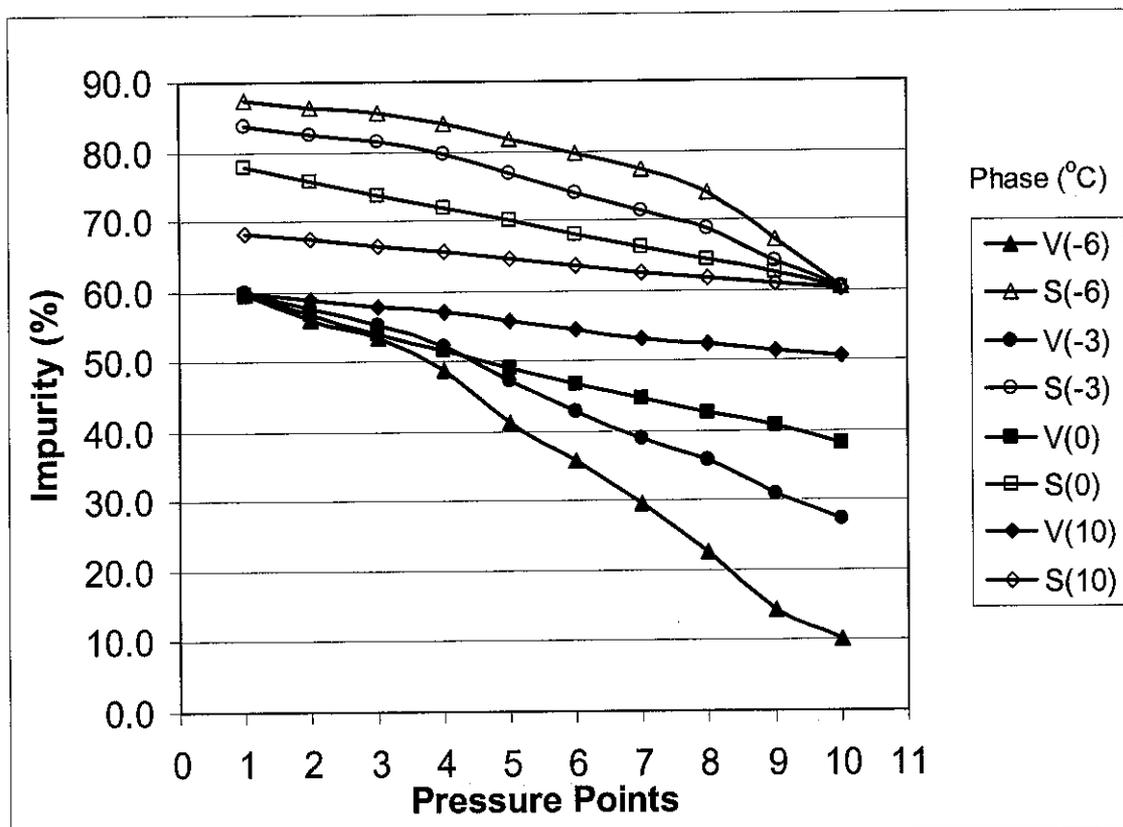
Figure A3.1: Phase impurity (%CO$_2$) versus temperature and pressure at 60% feed impurity. (K-chart Method)

Table A3.19: Phase compositions of CH$_4$ and CO$_2$ at -6°C and various pressures (40% Feed Impurity). (K-chart method)

P (kPa)	Vapor fraction	Solid fraction	CO$_2$ vapor %	CH$_4$ vapor %	CO$_2$ solid %	CH$_4$ solid %
365	0.99	0.01	39.8	60.2	81.2	18.8
400	0.81	0.19	31.3	68.7	78.1	21.9
440	0.70	0.30	25.0	75.0	75.3	24.7
490	0.62	0.38	19.8	80.2	72.3	27.7
560	0.53	0.47	15.2	84.8	68.3	31.7
630	0.46	0.54	12.1	87.9	64.2	35.8
710	0.39	0.61	9.6	90.4	59.2	40.8
800	0.29	0.71	7.6	92.4	53.1	46.9
900	0.14	0.86	5.8	94.2	45.5	54.5
960	0.01	0.99	4.9	95.1	40.4	59.6

Table A3.20: Phase compositions of CH_4 and CO_2 at -3°C and various pressures (40% Feed Impurity). (K-chart method)

P (kPa)	Vapor fraction	Solid fraction	CO_2 vapor %	CH_4 vapor %	CO_2 solid %	CH_4 solid %
973	0.99	0.01	39.6	60.4	71.7	28.3
1026	0.86	0.14	35.2	64.8	68.3	31.7
1079	0.75	0.25	31.5	68.5	64.9	35.1
1132	0.65	0.35	28.3	71.7	61.5	38.5
1185	0.56	0.44	25.4	74.6	58.2	41.8
1238	0.46	0.54	22.9	77.1	54.8	45.2
1291	0.37	0.63	20.6	79.4	51.4	48.6
1344	0.27	0.73	18.5	81.5	47.9	52.1
1397	0.15	0.85	16.5	83.5	44.2	55.8
1453	0.01	0.99	14.5	85.5	40.3	59.7

Table A3.21: Phase compositions of CH_4 and CO_2 at 0°C and various pressures (40% Feed Impurity). (K-chart method)

P (kPa)	Vapor fraction	Solid fraction	CO_2 vapor %	CH_4 vapor %	CO_2 solid %	CH_4 solid %
1742	0.99	0.01	39.9	60.1	61.8	38.2
1780	0.89	0.11	37.6	62.4	59.5	40.5
1820	0.78	0.22	35.3	64.7	57.1	42.9
1860	0.68	0.32	33.1	66.9	54.7	45.3
1900	0.58	0.42	31.0	69.0	52.3	47.7
1940	0.47	0.53	29.0	71.0	49.9	50.1
1980	0.37	0.63	27.1	72.9	47.5	52.5
2020	0.26	0.74	25.2	74.8	45.1	54.9
2060	0.14	0.86	23.4	76.6	42.6	57.4
2100	0.01	0.99	21.7	78.3	40.2	59.8

Table A3.22: Phase compositions of CH_4 and CO_2 at 10°C and various pressures (40% Feed Impurity). (K-chart method)

P (kPa)	Vapor fraction	Solid fraction	CO_2 vapor %	CH_4 vapor %	CO_2 solid %	CH_4 solid %
5050	0.99	0.01	39.9	60.1	50.1	49.9
5080	0.86	0.14	38.6	61.4	48.8	51.2
5110	0.73	0.27	37.3	62.7	47.5	52.5
5140	0.61	0.39	36.0	64.0	46.3	53.7
5170	0.49	0.51	34.8	65.2	45.1	54.9
5200	0.38	0.62	33.6	66.4	43.9	56.1
5230	0.26	0.74	32.4	67.6	42.7	57.3
5260	0.15	0.85	31.3	68.7	41.6	58.4
5290	0.04	0.96	30.2	69.8	40.4	59.6
5298	0.01	0.99	29.9	70.1	40.1	59.9
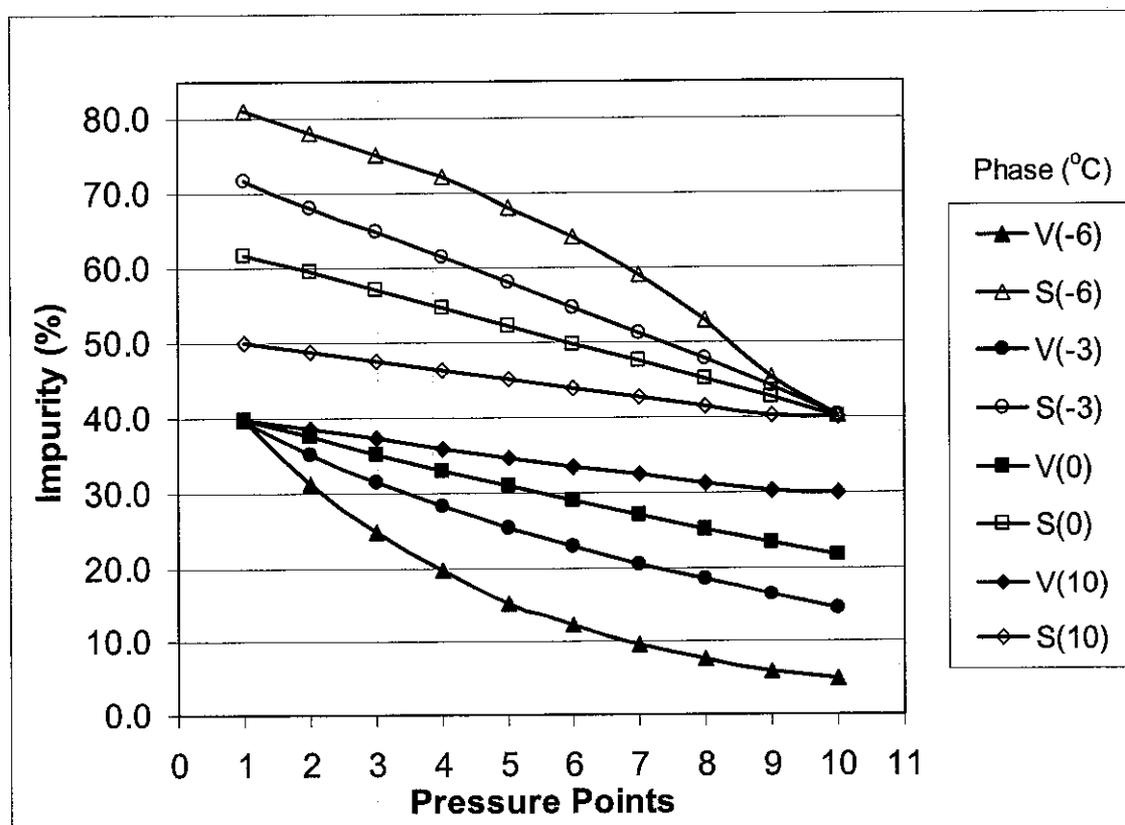
Figure A3.2: Phase impurity (%CO_2) versus temperature and pressure at 40% feed impurity. (K-chart Method)

Table A3.23: Phase compositions of CH_4 and CO_2 at -6°C and various pressures (10% Feed Impurity). (K-chart method)

P (kPa)	Vapor fraction	Solid fraction	CO_2 vapor %	CH_4 vapor %	CO_2 solid %	CH_4 solid %
724	0.99	0.01	9.3	90.7	58.3	41.7
880	0.91	0.09	6.1	93.9	47.1	52.9
1000	0.82	0.18	4.3	95.7	36.8	63.2
1090	0.72	0.28	3.1	96.9	28.0	72.0
1140	0.62	0.38	2.4	97.6	22.7	77.3
1190	0.46	0.54	1.7	98.3	17.0	83.0
1210	0.35	0.65	1.5	98.5	14.6	85.4
1220	0.28	0.72	1.3	98.7	13.4	86.6
1235	0.15	0.85	1.2	98.8	11.5	88.5
1246.5	0.01	0.99	1.0	99.0	10.1	89.9

Table A3.24: Phase compositions of CH_4 and CO_2 at -3°C and various pressures (10% Feed Impurity). (K-chart method)

P (kPa)	Vapor fraction	Solid fraction	CO_2 vapor %	CH_4 vapor %	CO_2 solid %	CH_4 solid %
1595	0.99	0.01	9.9	90.1	29.7	70.3
1620	0.95	0.05	9.1	90.9	27.7	72.3
1660	0.87	0.13	7.9	92.1	24.4	75.6
1700	0.77	0.23	6.7	93.3	21.0	79.0
1740	0.63	0.37	5.5	94.5	17.6	82.4
1780	0.41	0.59	4.3	95.7	14.0	86.0
1800	0.25	0.75	3.7	96.3	12.1	87.9
1810	0.15	0.85	3.4	96.6	11.2	88.8
1815	0.10	0.90	3.2	96.8	10.7	89.3
1822	0.01	0.99	3.0	97.0	10.1	89.9

Table A3.25: Phase compositions of CH_4 and CO_2 at $0^\circ C$ and various pressures (10% Feed Impurity). (K-chart method)

P (kPa)	Vapor fraction	Solid fraction	CO_2 vapor %	CH_4 vapor %	CO_2 solid %	CH_4 solid %
2399	0.99	0.01	9.9	90.1	20.4	79.6
2410	0.95	0.05	9.5	90.5	19.7	80.3
2450	0.78	0.22	8.0	92.0	16.8	83.2
2470	0.67	0.33	7.3	92.7	15.4	84.6
2490	0.53	0.47	6.6	93.4	13.9	86.1
2500	0.46	0.54	6.2	93.8	13.2	86.8
2510	0.37	0.63	5.8	94.2	12.4	87.6
2520	0.27	0.73	5.5	94.5	11.7	88.3
2530	0.16	0.84	5.1	94.9	10.9	89.1
2542	0.01	0.99	4.7	95.3	10.0	90.0

Table A3.26: Phase compositions of CH_4 and CO_2 at $10^\circ C$ and various pressures (10% Feed Impurity). (K-chart method)

P (kPa)	Vapor fraction	Solid fraction	CO_2 vapor %	CH_4 vapor %	CO_2 solid %	CH_4 solid %
6095	0.99	0.01	9.9	90.1	16.2	83.8
6120	0.92	0.08	9.5	90.5	15.6	84.4
6150	0.83	0.17	9.0	91.0	14.9	85.1
6190	0.71	0.29	8.4	91.6	14.0	86.0
6230	0.58	0.42	7.7	92.3	13.1	86.9
6270	0.43	0.57	7.1	92.9	12.2	87.8
6300	0.31	0.69	6.7	93.3	11.5	88.5
6330	0.18	0.82	6.3	93.7	10.8	89.2
6350	0.09	0.91	6.0	94.0	10.4	89.6
6367	0.01	0.99	5.7	94.3	10.0	90.0
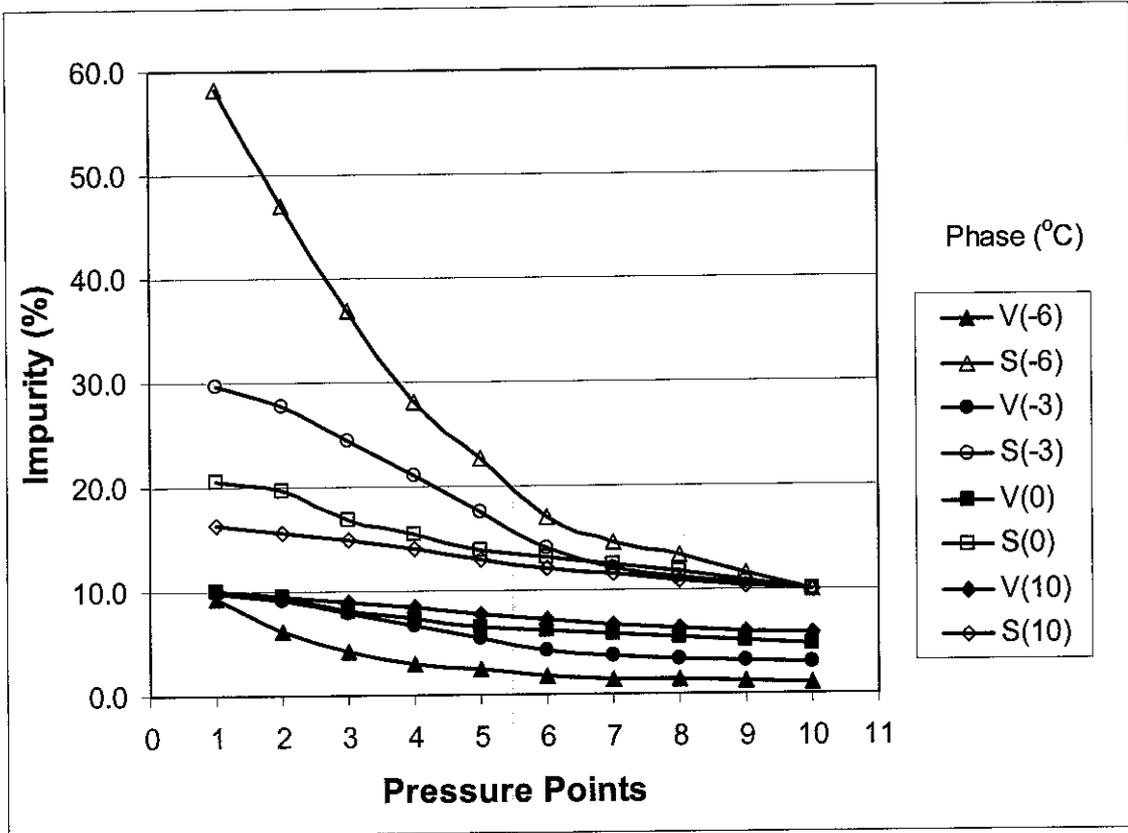
Figure A3.3: Phase impurity (%CO₂) versus temperature and pressure at 10% feed impurity. (K-chart Method)

REFERENCES

1. Sloan E.D.Jr. (1998) Clathrate Hydrates of Natural Gases, 2nd. New York: Marcel Dekker.

2. Hollander F. and JeffreyG.A. (1977) J. Chem. Phys., 66, 4699-4705.

3. Von Stackelberg M. (1949) Naturwissenshaften, 36, 327-333.

4. Spillman, R.W., 1989, Chem. Eng. Progr. 85,41.

5. Rojey, A., Jaffaret, C., Cornot-Gandolphe, S., Durand, B., Julian, S. and Valais, M., 1997, Natural Gas Production Processing Transport, Editions Technip, Paris.

6. Alexei V. Milkov, 2003. Global estimates of hydrate-bound gas in marine sediments: how much is really out there?. BP America, Exploration and Production Technology Group, 501 Westlake Park Boulevard, Houston, TX 77079, USA. A.V. Milkov / Earth-Science Reviews 66 (2004) 183–197 197.

7. Michael J. Moran and Howard N. Shapiro, "Fundamentals of engineering thermodynamics", 4th edition, 552-555.

8. C.N. Murray, L. Visintini, G. Bidoglio, B. Henry, "Permanent storage of carbon dioxide in the marine environment: the solid CO_2 penetrator", 1995